TECTONICS, VOL. 21, NO. 3, 1016, 10.1029/2001TC901032, 2002

Archean granite-greenstone tectonics at Kolar (South India): Interplay of diapirism and bulk inhomogeneous contraction during juvenile magmatic accretion

Dominique Chardon,[1] Jean-Jacques Peucat,[2] Mudlappa Jayananda,[3] Pierre Choukroune,[1] and C. Mark Fanning[4]

Received 1 August 2001; revised 27 December 2001; accepted 4 February 2002; published 15 June 2002.

[1] The structural study of the Kolar greenstone belt and surrounding granite-gneiss terrains combined with U-Pb dating reveals that the middle and lower crustal tectonoplutonic pattern of the eastern Dharwar craton developed during a major magmatic accretion event between 2550 and 2530 Ma. The granite-greenstone pattern resulted from the interference of gravity-driven sagging of the greenstones (i.e., diapirism), E-W bulk inhomogeneous shortening combined with horizontal N-S stretching, and syntectonic juvenile pluton emplacement. Bulk inhomogeneous contraction is accommodated by the synchronous development of a pervasive, N-S trending vertical foliation, shallow stretching lineation, and conjugate strike-slip shear zone pattern within and outside the greenstone belt, resulting in regional horizontal pure shear deformation. The plutons around the greenstone belt record regional contraction by developing one set of strike-slip C-S fabrics of the shear zone pattern. The development of the granite-greenstone pattern was coeval and compatible with deformation during juvenile magmatic accretion, melting, and granulite metamorphism in the lower crust. The Kolar example points to a specific crustal rheology that allowed sagduction of the greenstones and regional distributed bulk inhomogeneous strain, due to mechanical homogeneity and low viscosity provided by large-scale melting during the accretion event. This example further suggests specific boundary conditions to the craton that allowed E-W inhomogeneous shortening to be accommodated by N-S stretching and spreading of the crust without significant tectonic thickening. Such tectonoplutonic pattern is specific to the Archean and may develop as a consequence of mantle plume activity in intracontinental settings. *INDEX TERMS:* 8110 Tectonophysics: Continental tectonics—general (0905); 8099 Structural Geology: General or miscellaneous; 9619 Information Related to Geologic Time: Precambrian; 8035 Structural Geology: Pluton emplacement; 8199 Tectonophysics: General or miscellaneous; *KEYWORDS:* greenstone belt, continental deformation, pluton emplacement, granulite, shear zones

1. Introduction

[2] Granite-greenstone tectonics is almost systematically synchronous with large-scale crustal melting and voluminous plutonism. This plutonism is mainly characterized by the production of tonalite, trondhjemite, and granodiorite (TTG)-type magmas resulting from partial melting of tholeiitic basalts turned into garnet-bearing amphibolites or hornblende eclogites [*Martin*, 1994]. This magmatism coeval with granite-greenstone tectonism is juvenile, i.e., the crystallization age of the magma (U-Pb zircon age) is very close to or coincides with the extraction age of its mafic protolith from the mantle (Nd model age). Such magmatism therefore contributes to crustal growth by addition of newly mantle-derived material to the continental crust.

[3] The transposition of modern-like plate tectonics scenarios to Archean terrains (i.e., actualism) prevails in the literature. In Archean provinces where the greenstone belts' mafic volcanics show no or little evidence of interaction with preexisting continental crust, lateral tectonic accretion of new segments of crust in the form of continental or island arcs or back arc terranes is emphasized, whereas diapiric granite-greenstone tectonics [*Jelsma et al.*, 1993; *Bouhallier et al.*, 1995; *Chardon et al.*, 1996, 1998; *Collins et al.*, 1998] appear to take place in provinces where greenstone belts' mafic volcanics are emplaced in a preexisting segment of continental crust, implying dominantly gravity-driven recycling of continental crust during juvenile magmatic underaccretion. *Choukroune et al.* [1997] suggested that those two tectonomagmatic scenarios might apply to a same portion of Archean continental lithosphere at different stages of its development (i.e., primitive lateral accretion and later intracontinental reworking and vertical juvenile accretion).

[4] The Kolar greenstone belt (KGB) in the eastern Dharwar craton, South India, provides a particularly relevant case study for testing models of Archean tectonics and continental growth. Indeed, a considerable geochemical

[1]Centre Européen de Recherche et d'Enseignement de Géosciences de l'Environnement (UMR CNRS 6635), Université Aix-Marseille 3, Aix-en-Provence, France.
[2]Géosciences-Rennes (UMR CNRS 6118), Université Rennes 1, Campus de Beaulieu, Rennes Cedex, France.
[3]Department of Geology, Bangalore University, Bangalore, India.
[4]Research School of Earth Sciences, Australian National University, Canberra ACT, Australia.

0278-7407/02/2001TC901032

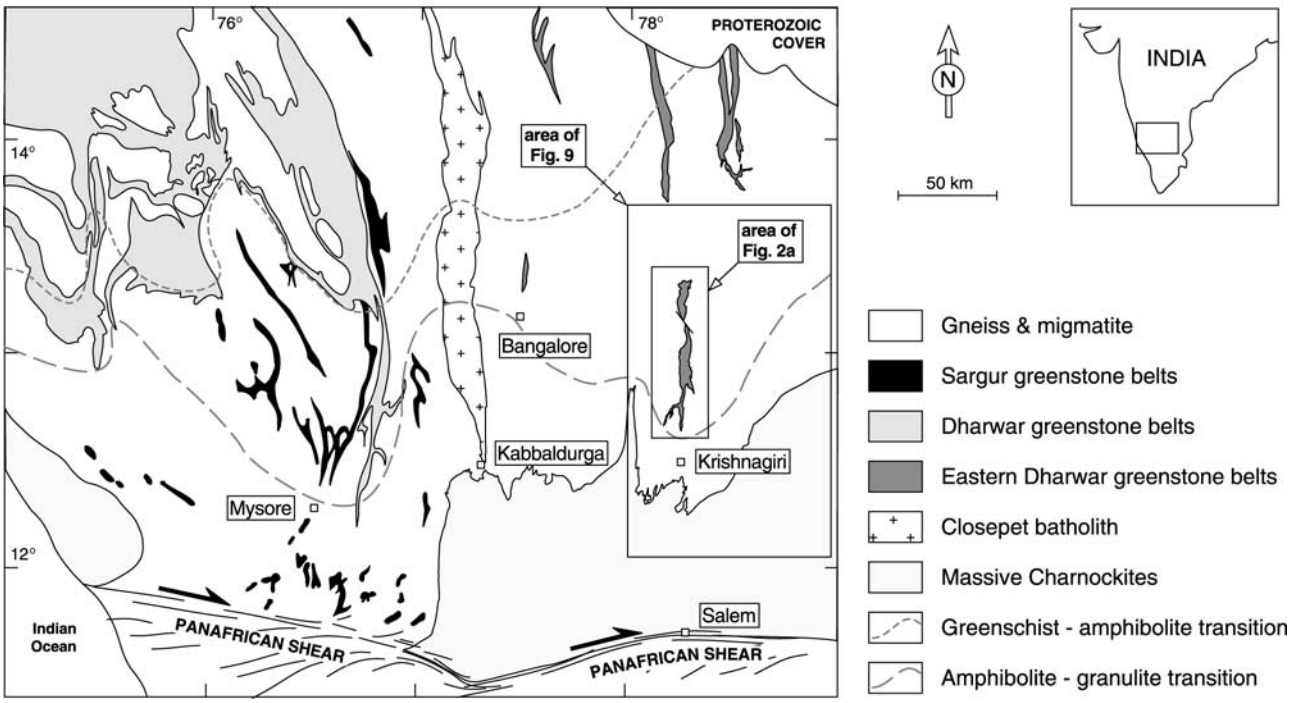

Figure 1. Geological map of the Southern Dharwar craton, partly adapted from *Drury et al.* [1984], *Raase et al.* [1986], *Bouhallier et al.* [1995], and the present work.

data set is available from the greenstones and their adjoining granite-gneiss rocks [e.g., *Rajamani et al.*, 1987; *Walker et al.*, 1990; *Balakrishnan et al.*, 1990], indicating voluminous late Archean magmatic accretion around the belt [*Krogstad et al.*, 1989, 1991, 1995]. On the basis of the contrasted geochronological record in the gneisses from both sides of the KGB, the belt has been interpreted as a modern-like suture zone between an old (>3 Gyr) western continent and a 2.5-Gyr-old eastern juvenile magmatic arc [*Krogstad et al.*, 1989, 1995]. However, so far, local structural observations made in the KGB and its surrounding rocks [*Mukhopadhyay and Haimanot*, 1989; *Mukhopadhyay*, 1990] argue for limited horizontal tectonic displacement or thrusting in the vicinity of the greenstone belt.

[5] Here we present the results of an integrated study of the greenstone belt and neighboring granite-gneiss terrains on the basis of extensive strain fabrics mapping and sensitive high-resolution ion microprobe (SHRIMP) U-Pb dating of synkinematic plutons (sections 4 and 5) to characterize the tectonic context of development of the Kolar granite-greenstone pattern. We also present a structural investigation from the greenstone belt to lower structural levels (section 6) in order to evaluate the spatial and temporal relations between deformation and lower crustal juvenile accretion and granulite metamorphism. We show that the three-dimensional middle and lower crustal strain pattern developed between 2550 and 2530 Myr ago as a result of the interference of diapirism between the greenstones and their basement and regionally distributed inhomogeneous shortening during voluminous juvenile magmatic accretion, crustal melting, and granulite metamorphism. We argue that such tectonic process is specific to the Archean and was facilitated by mantle plume activity (section 7).

2. Geology of the Dharwar Craton

[6] A continuous section of late Archean continental crust is exposed in the Dharwar craton (Figure 1). As a result of a Phanerozoic solid-body tilt of the craton, deepest granulitic crustal levels (8–9 kbar) are exposed in the south, while low-grade rocks (2–3 kbar) [*Raase et al.*, 1986] crop out in the north. Typical Archean TTG-greenstone lithologies make up most of the crustal section. TTG series are 3.4 to 2.5 Gyr old and have been grouped under the term ''peninsular gneiss complex'' (for reviews, see *Peucat et al.* [1993a, 1995], *Jayananda et al.* [2000], and *Chadwick et al.* [2000]).

[7] Greenstone belts are divided into three groups on the basis of their stratigraphy and age [*Swami Nath et al.*, 1976; *Swami Nath and Ramakrishnan*, 1981] (Figure 1). In the western part of the craton, older (3.3–3.0 Ga) Sargur Group greenstone belts are deformed together with the Peninsular gneisses at medium- to high-grade metamorphic conditions and are unconformably overlaid by the younger (3.02–2.52 Ga) moderately deformed Dharwar Supergroup greenstone belts [*Peucat et al.*, 1995; *Nutman et al.*, 1996; *Trendall et al.*, 1997a, 1997b]. Gold-bearing greenstone belts from the eastern Dharwar craton (i.e., Kolar-type greenstone belts) are partly coeval with the Dharwar Supergroup greenstone belts [*Walker et al.*, 1990; *Nutman et al.*, 1996; *Balakrishnan et al.*, 1999; *Vasudev et al.*, 2000]. However, they differ from the latter with respect to the importance of the

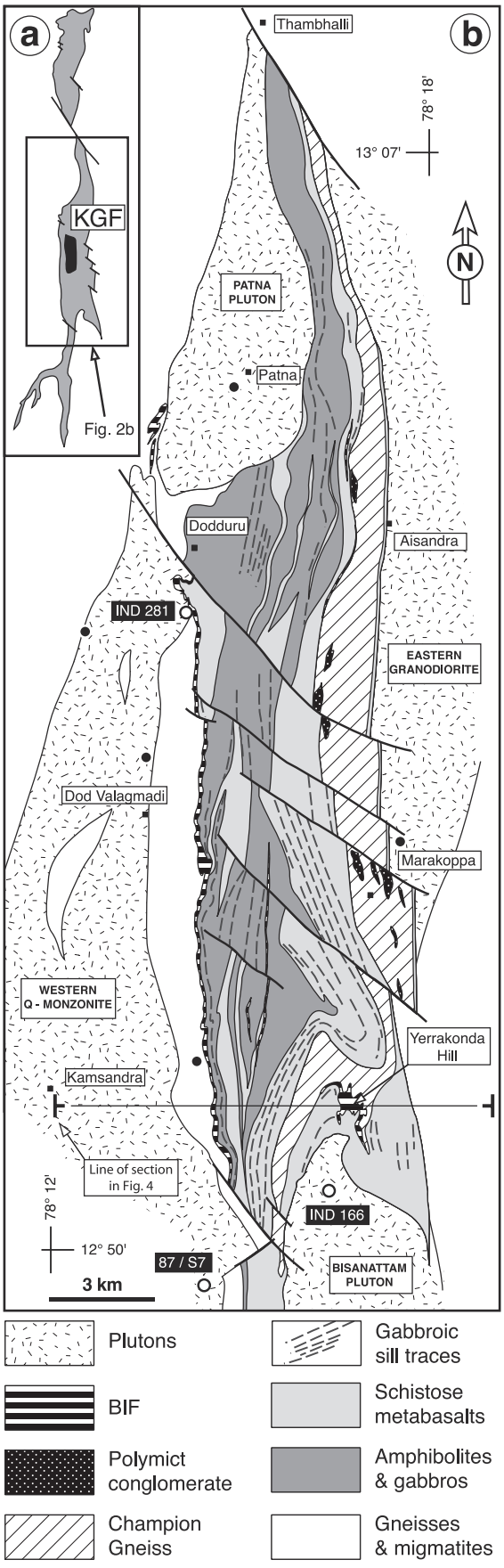

sedimentary component, which is very low compared to the Dharwar Supergroup greenstone belts.

[8] The development of the dominantly N-S structural grain of the craton and the emplacement of the Closepet batholith (Figure 1) were coeval with regional partial melting and granulite peak metamorphism at around 2.5 Ga [*Drury et al.*, 1984; *Friend and Nutman*, 1991; *Peucat et al.*, 1993a; *Bouhallier*, 1995; *Choukroune et al.*, 1995]. To the east of the Closepet batholith, numerous plutonic bodies were emplaced during the late Archean tectonometamorphic episode. This juvenile magmatism represents substantial crustal accretion, with melts (including the Closepet) displaying various degrees of interaction with preexisting crust [*Peucat et al.*, 1989, 1993a; *Krogstad et al.*, 1991, 1995; *Jayananda et al.*, 1995, 2000; *Moyen et al.*, 2001].

[9] Two broad classes of interpretations of the late Archean granite-greenstone pattern have been proposed. Actualistic models, essentially based on numerous petrological/geochemical studies and fewer structural works, invoke nappe tectonics and/or folding of greenstone belts and their basement rocks in a context of N-S continental collision [*Drury et al.*, 1984], subduction [*Newton*, 1990], or active margin tectonics during dominant E-W convergence [*Krogstad et al.*, 1989; *Chadwick et al.*, 2000]. A nonactualistic model argues for the intracontinental development of diapiric instabilities between the greenstones and the granite-gneiss terrains interfering with E-W contraction and strike-slip shearing in the western Dharwar craton at around 2.5 Ga [*Choukroune et al.*, 1995]. This model is based on studies of kinematic relationships between Sargur-type or Dharwar-type greenstone belts and their surrounding granite-gneiss terrains [*Bouhallier et al.*, 1993, 1995; *Chardon et al.*, 1996, 1998]. The thermomechanical context of development of such gravity instabilities suggested by physical modeling [*Chardon*, 1997; 1998; *Mège et al.*, 2000], together with petrological and isotopic studies, is used to propose that plume activity could have enhanced juvenile underplating, pluton emplacement, crustal melting, and diapiric instabilities during E-W shortening of the craton [*Peucat et al.*, 1993b; *Choukroune et al.*, 1995, 1997; *Jayananda et al.*, 1995, 2000].

3. Geology of the Kolar Greenstone Belt and Surrounding Basement Rocks

[10] *Viswanatha* [1978] and *Viswanatha and Ramakrishnan* [1981] gave a detailed geological description of the KGB that can be summarized as follows. The dominant rock type in the belt belongs to a komatiitic/tholeiitic volcanic complex that was transformed into amphibolites (Figure 2). Pillow basalts are largely developed, suggesting

Figure 2. (opposite) (a) Sketch map of the Kolar greenstone belt showing the town of Kolar Gold Fields (KGF) and the study area. (b) Geological map of the central Kolar greenstone belt and its neighboring granite-gneiss terrains (after *Viswanatha* [1978] and the present work). Solid dots refer to zircon U-Pb geochronological samples of *Krogstad et al.* [1991]. Open dots refer to samples dated in this study.

subaqueous environment eruption conditions. This rock unit contains sills of porphyritic basalt or gabbro and bands of metapyroxenite. The term ''Champion Gneiss'' describes a formation dominated by felsic metagreywakes and volcanics that makes up the eastern part of the belt. The Champion Gneiss has numerous lenses of what has been described as a conglomerate (Figure 2), which contains subrounded to angular clasts of granitoids, migmatitic gneisses, and greenstones in a fine quartzo-feldspathic matrix. Banded iron formations (BIF) mark the western contact of the belt and form most of Yerrakonda Hill (Figure 2). Thin concordant BIF layers are scattered throughout the belt. The age of the volcanic complex is not well constrained. *Walker et al.* [1990] obtained 2.7−2.4 Ga Rb-Sr whole rock isochron ages for some amphibolites from the eastern KGB and retained a 3 point isochron age at 2710 ± 48 Ma, while a Pb-Pb whole rock isochron age of 2732 ± 155 Ma was obtained on metabasalts from the western part of the belt [*Balakrishnan et al.*, 1990].

[11] Basement rocks west of the greenstone belt are represented by a gneiss complex that is intruded by a large porphyritic and foliated plutonic body [*Viswanatha*, 1978], called hereinafter the western quartz-monzonite, after the work of *Jayananda et al.* [2000] (Figure 2). Zircon U-Pb dating of the banded gneisses close to the western boundary of the KGB (Figure 2) by *Krogstad et al.* [1991] yielded a minimum age of 3140 Ma. Following *Balakrishnan and Rajamani* [1987], *Krogstad et al.* [1991] have considered two intrusive generations of gneiss (Dod- and Dosa-type) in the gneiss complex west of the KGB. The detailed work of *Viswanatha* [1978], our own structural mapping, and the description and location of the Dod and Dosa gneiss samples dated by *Krogstad et al.* [1991] suggest that those two gneiss types are, in fact, two facies of the western quartz-monzonite. Indeed, the Dod and Dosa gneisses are K-feldspar porphyritic monzodioritic and granodioritic ''gneisses,'' respectively (*Krogstad et al.* [1991], data repository) that are clearly distinguishable from the nonporphyritic gray gneisses seen outside the pluton. The Dod and Dosa facies yielded U-Pb zircon ages of 2631 and 2610 Ma, respectively [*Krogstad et al.*, 1991] (Figure 2), with some inheritance (>2800 Ma). In the southern part of the study area (sample 87/S7, Figure 2), the western quartz-monzonite has a U-Pb zircon evaporation age of 2552 ± 2 Ma and contains inherited zircons up to 2850 Myr old [*Jayananda et al.*, 2000]. Those results, together with isotopic data from the pluton and gneissic country rocks, suggest that the western quartz-monzonite is a juvenile magma contaminated by the surrounding old (>3000 Ma) crust [*Krogstad et al.*, 1991, 1995]. The Patna pluton is mainly granodioritic in composition and has undergone the same petrogenetic evolution as the western quartz-monzonite [*Balakrishnan and Rajamani*, 1987; *Krogstad et al.*, 1995]. This pluton yielded a U-Pb zircon age of 2551 ± 2 Ma [*Krogstad et al.*, 1991] (Figure 2).

[12] East of the KGB, migmatites are in contact toward the west with a N-S elongate granodioritic body that bounds the greenstone belt (called hereinafter the eastern granodiorite) (Figure 2). This foliated pluton yielded a 2532 ± 3 Ma U-Pb zircon age [*Krogstad et al.*, 1991] (who described it as a ''Kambha gneiss'') and its isotopic composition suggests a slightly depleted mantle source [*Jayananda et al.*, 2000] with no crustal contamination [*Krogstad et al.*, 1995]. East of the eastern granodiorite, some gneissic enclaves in the migmatites have circa 2.7-Gyr-old zircons (J.-J. Peucat et al., manuscript in preparation).

[13] The central KGB is a complex upright synform that is perturbed in the north and in the south by the emplacement of the Patna and Bisanattam plutons, respectively (Figure 2). It is cut by late, en echelon NW striking chisel faults [*Viswanatha*, 1978]. The KGB records lower amphibolite facies metamorphic conditions, with an increase of the metamorphic grade toward its contacts, especially in the vicinity of the plutons [*Viswanatha and Ramakrishnan*, 1981].

4. Structural Analysis, Central Kolar Greenstone Belt

4.1. Strain Fabrics

[14] On both sides of the KGB, foliations in the migmatites, gneisses, and plutons strike consistently north to NNE (Figures 3a). West of the belt, the foliations are dominantly steeply dipping east and acquire more pronounced NNE strikes toward the north, within and west of the Patna granite (Figures 3a and 4). Foliations within this pluton are broadly parallel to those in the gneisses and in the KGB. From Dodduru to the south, the foliation in the gneisses tends to parallel the western margin of the belt in the vicinity of the granite-greenstone contact (Figures 3 and 4). There, the gneisses and the northeasternmost part of the western quartz-monzonite are involved in a 500- to 800-m-thick mylonite zone bounding the KGB that was first reported by *Rajamani et al.* [1987]. This W-E strain gradient is marked by the development of a plastic foliation that is accompanied by intense grain size reduction of the orthogneisses and plutonic rocks. East of the KGB, moderately west dipping foliations acquire steeper dips at the contact with the belt, where they parallel foliations in the greenstones (Figures 3a and 4). South of the KGB the pervasive foliation within the Bisanattam pluton is invariably subvertical and N-S striking.

[15] Synkinematic metamorphic minerals such as hornblende, chlorite, or plagioclase define a single foliation throughout the KGB. The steeply east dipping to vertical foliation in the BIF at the western margin of the belt parallels the contact and the mylonitic foliation in the orthogneisses. The foliation keeps this orientation within the western half of the KGB. Further east, the foliation is moderately to steeply west dipping. This simple inward convergent foliation pattern is slightly disturbed in the northern and southern parts of the study area (Figure 4). In the Yerrakonda Hill area (Figures 2 and 3a), foliation trajectories display a convex bend toward the east in the vicinity of map-scale folds underlined by the Champion Gneiss formation. Further south, the foliation is either N-S striking or parallel to the granite-greenstone contact. The

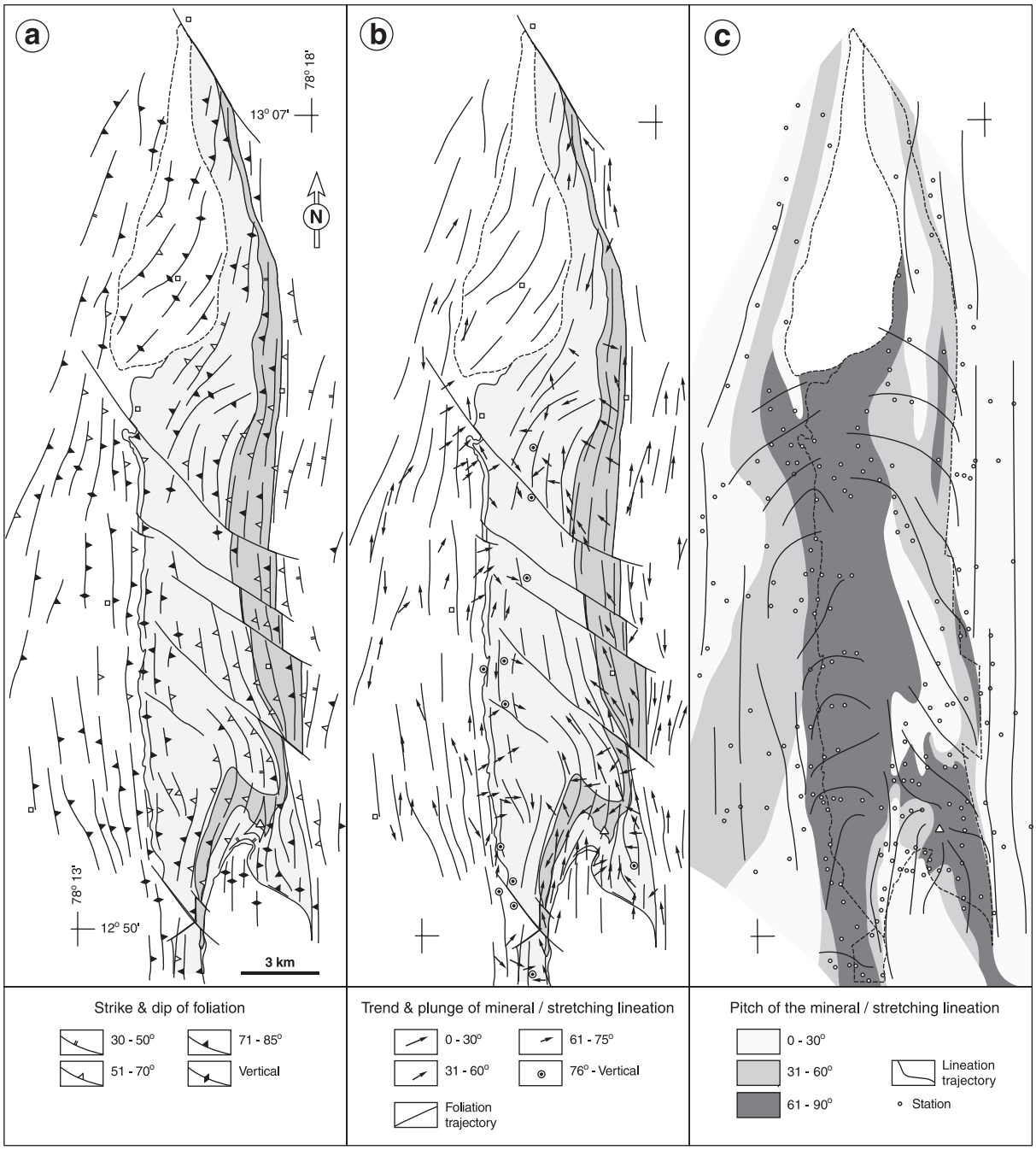

Figure 3. Strain fabrics maps of the central Kolar greenstone belt and its neighboring granite-gneiss terrains. (a) Foliation trajectories (the Yerrakonda Hill triple point is shown); (b) mineral-stretching lineation measurements; (c) contours of the pitch values of the mineral-stretching lineations and lineation trend lines.

interference between dominantly N-S trending and pluton boundary-parallel foliations defines a foliation triple point in the southeastern part of the KGB (Figure 3a). In the northern part of the study area the foliation is deflected in the vicinity of the Patna pluton.

[16] Mineral-stretching lineations are subhorizontal to shallowly plunging in the granite gneiss terrains, except within the mylonitic orthogneisses at the western margin of the KGB (Figure 3b). From west to east, toward and within the mylonite zone, the pitch of the lineation drastically increases, and its azimuth varies from north to east (Figures 3b, 3c, and 4). Within the KGB, the mineral-stretching lineation is expressed by the alignment of hornblende crystals, chlorite flakes, and stretched amygdales. In the western part of the belt, the lineation parallels the finite stretching direction in the mylonitic orthogneiss at the

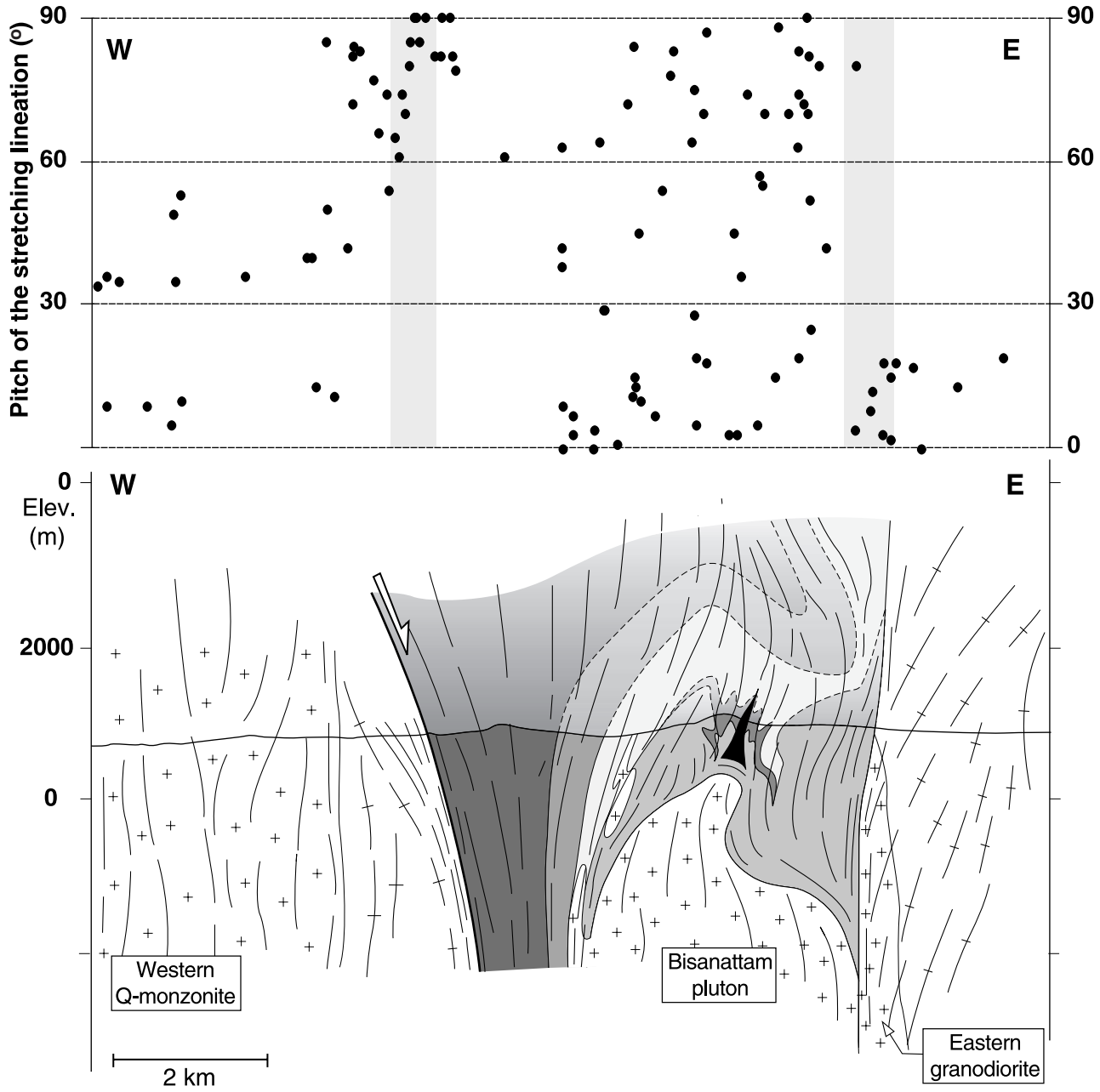

Figure 4. E-W section across the Kolar greenstone belt (line of section is located on Figure 2b) and corresponding lineation pitch transect (taking into account measurement sites located south of Dod Valagmadi; Figure 2b). Thin lines represent the foliation trace. The Yerrakonda Hill foliation triple point is also shown. Shaded areas on the pitch transect mark the boundaries of the greenstone belt. For geological caption, see Figure 2b.

contact and remains E-W trending and almost downdip in the western half of the belt (Figures 3b, 3c, and 4). In the eastern part of the belt, lineations are dominantly shallowly to moderately plunging to the northwest, with intermediate pitches. In the southern part of the study area the lineation pattern is more complex (Figures 3b, 3c,, and 4). West of Yerrakonda Hill, a N-S elongate zone of horizontal to shallowly north plunging lineations stretches from the western and northwestern contact of the Bisanattam pluton into the interior of the belt. SE of Yerrakonda Hill, the lineations trend perpendicular to the granite-greenstone contact and are steeply plunging toward the interior of the belt.

[17] Shape fabrics in the gneisses, plutons, and greenstones are of LS type, suggesting general plain strain conditions throughout the study area. In the vicinity of the Yerrakonda Hill foliation triple point, the greenstones and ferruginous quartzites show constrictive fabrics (Figures 2 and 3). In this

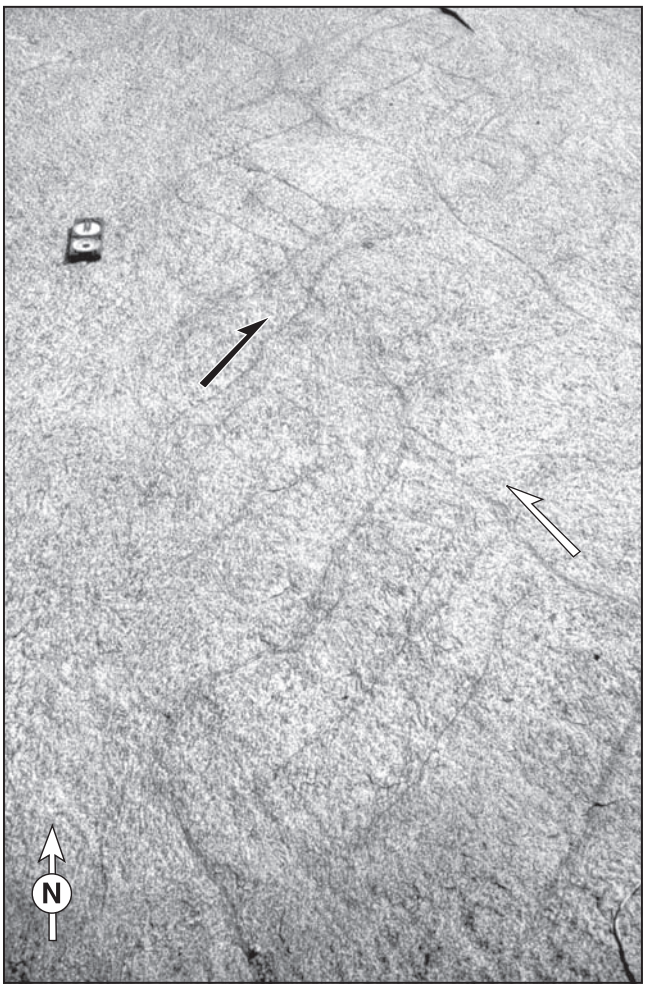

Figure 5. Conjugate, anastomosed shear zones in the migmatitic gneisses east of the KGB. Shearing was taking place at the time the gneiss was partially molten. Leucomelts were expelled from the shear zone network during shearing. This resulted in a concentration of restitic material in the shear zones (3 km SE of Marakoppa; Figure 2b).

area, lineation trend lines are radial and converge toward the foliation triple point (Figures 3a and 3c).

4.2. Granite-Greenstone Relations, Superimposed Strain Patterns, and Kinematics

4.2.1. Western boundary of the belt

[18] The mylonitic fabric affecting the basement rocks and the western quartz-monzonite along the western margin of the KGB is superimposed on preexisting high-temperature subsolidus planar and linear fabrics. The sharp reorientation of the stretching direction across the strain gradient is associated with the activation of deformation mechanisms of lower temperature (grain size reduction) than those that presided to the growth and stabilization of the preexisting fabrics. Seven out of eleven thin sections of the mylonitic orthogneiss reveal east side down kinematics. Noncoaxial deformation features are C' shear bands bounding sigma-shaped feldspar porphyroclasts and associated with the synkinematic development of biotite and, eventually, muscovite, where the deformation is most intense. In the four remaining thin sections, shear sense determination is not possible or ambiguous given the absence of feldspar porphyroclasts and/or intense dynamic recrystallization of quartz. The pervasive planar and linear fabrics in the BIF forming the western margin of the KGB and fabrics in the mylonite are parallel. The continuity of these fabrics into the amphibolites further east within the KGB (Figures 3a and 3b) suggests that the strain pattern developed in the western part of the KGB and its adjoining gneisses and pluton through the mylonite results from a single deformation episode involving downward displacement of the greenstone with respect to the gneisses.

4.2.2. Pervasive regional strike-slip shearing

[19] In the granite-gneiss terrains adjoining the KGB to the east and to the west, the consistent attitude of the planar and linear fabrics argues for a simple regional deformation episode that affected every rock type. Superimposed on, or associated with, these fabrics are multiscale conjugate transcurrent shear zones affecting the granite-gneiss terrains and the KGB. The sinistral set of shear zones is NW trending, and the conjugate dextral set of shear zones is NE trending (Figures 5 and 6). This shear zone pattern is pervasive and distributed throughout the study area.

[20] Within the plutons emplaced around and against the KGB, transcurrent shearing is generally associated with strike-slip C-S fabrics, i.e., microscale associations of pervasive foliation and ductile shear bands produced by simple shearing of granitoid rocks during their cooling [*Berthé et al.*, 1979], as developed in typical syntectonic plutons [*Gapais*, 1989]. These C-S fabrics are compatible with either regional set of shear bands (Figure 6). The Bisanattam pluton displays pervasive dextral C-S fabrics on every visited outcrop. This is also observed in every meter-scale intrusion (mainly sill) of this pluton within the KGB west of Yerrakonda Hill, precisely where shallowly plunging, N-S trending stretching lineations occur (Figures 3b, 4, and 6) (note that those intrusions are not shown in Figures 2 and 6 because of their very small size).

[21] Pervasive sinistral C-S fabrics are seen on every outcrop of the eastern granodiorite (Figure 6). West of the KGB, dextral C-S fabrics are well developed in the northern part of the western quartz-monzonite (Figures 2 and 6). Locally, the Patna granite is affected by centimeter- to decimeter-wide, strike-slip shear zones that developed C-S fabrics (Figure 6). It is worth noting (1) that where both dextral C-S fabrics and sinistral shear bands are present in the study area, sinistral shearing systematically outlasts the development of the dextral C-S fabrics and (2) that dextral and sinistral C-S fabrics are not seen in the same pluton.

[22] East of the KGB the migmatites display equally developed sets of synmelt, dextral, and sinistral shear bands that are generally anastomosed (Figure 5). Toward the KGB, where these migmatites grade into the eastern granodiorite, the sinistral set becomes dominant. In the gneisses west of the KGB, the shear bands are ductile to brittle-ductile [see also *Mukhopadhyay and Haimanot*, 1989].

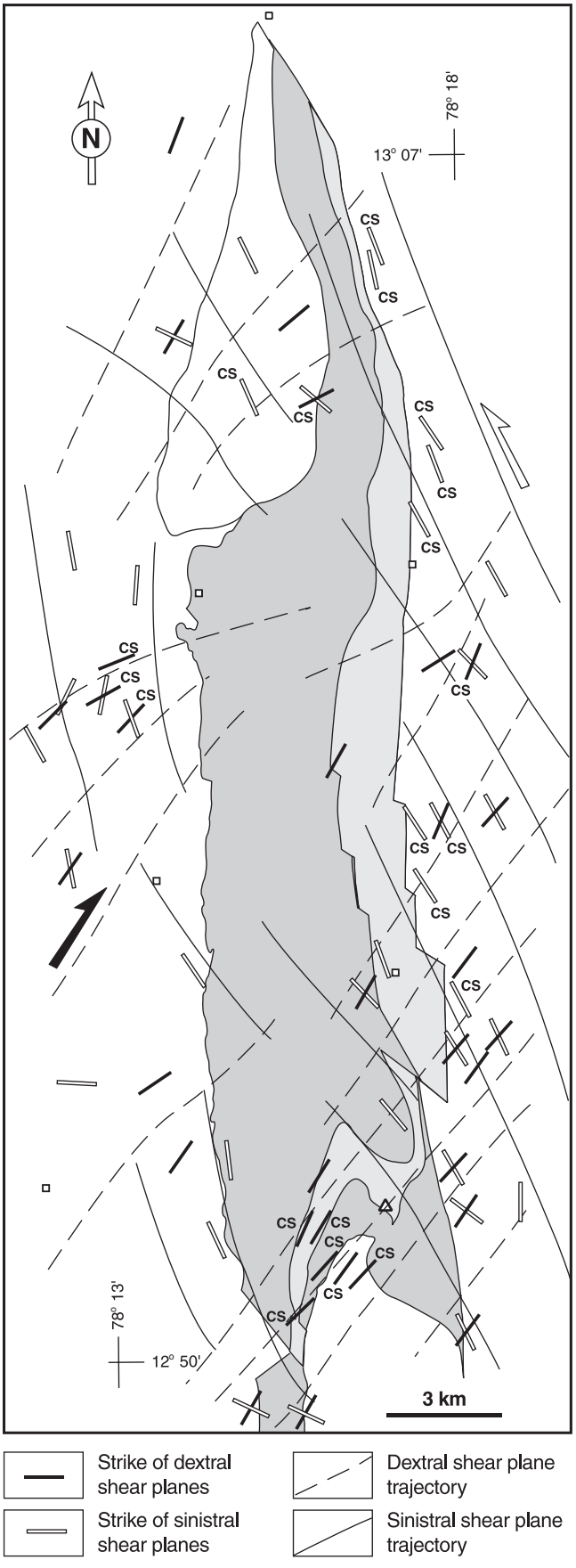

[23] Both sets of shear zones are observed within the metabasites of the KGB. Given the limited size and the bad quality of most outcrops, our mapping did not allow documentation of many conjugate structures. They are, however, widespread in underground mines where they control the localization of gold mineralization [*Hamilton and Hodgson*, 1986]. Considerable attention has been paid to the small-scale structures developed within the western BIF of the belt [*Ghosh and Sengupta*, 1985; *Mukhopadhyay*, 1989, 1990]. As they pointed out, the fold pattern is complex in the BIF. However, the consistent downdip orientation of the pervasive synmetamorphic stretching lineation throughout the BIF and adjoining amphibolites (Figure 3b) indicates that the main deformation event is associated with dip-slip shearing at the gneiss-greenstone contact. A late subhorizontal lineation is locally superimposed on the first lineation and is characterized by striations or by the preferred orientation of quartz fibers on foliation surfaces. Both sets of conjugate strike-slip shear bands were recognized in the BIF and are associated with the development of the latest folds [e.g., *Mukhopadhyay*, 1989]. Field relations suggest that the second lineation developed during conjugate strike-slip shearing superimposed on the earlier fabric. At several locations along the western contact, the strike-slip shear bands are superimposed on the mylonitic orthogneiss.

[24] The statistical analysis of all shear bands measured in the study area allows an estimation of the orientations of the principal axes of a regional bulk strain ellipsoid. The λ_1 is horizontal and N-S trending, and λ_3 is horizontal and E-W trending, while λ_2 is vertical (Figure 7). This is in agreement with the results of *Mukhopadhyay and Haimanot* [1989], who first described and characterized the conjugate sets of strike-slip shear zones in two quarries located on both sides of the KGB. The rather planar shape of the shear zones, as well as the good clustering of each set of conjugate shear directions, further suggests E-W regional bulk inhomogeneous crustal shortening with boundary conditions close to horizontal plane strain [*Gapais et al.*, 1987].

4.2.3. Granite-greenstone relations and pluton emplacement

[25] Pervasive C-S fabrics affect the Bisanattam pluton and the numerous small-scale intrusions of this pluton into the KGB in the Yerrakonda Hill area (Figure 6). The pluton's internal foliation parallels foliations in the KGB at their contact. These features show that the Bisanattam pluton is a typical syntectonic pluton [*Brun and Pons*, 1981; *Gapais*, 1989]. More precisely, the pluton has interfered with regional simple shearing, E-W regional contraction, and the early deformation pattern of the greenstone belt during its emplacement and cooling to produce the strain and folding interference pattern in the southeastern part of the central KGB (Figures 3 and 4). Constriction in this area is interpreted to result from the interference between Bisa-

Figure 6. (opposite) Distribution of strike-slip shear bands in the Kolar Gold Fields area and their trajectories. C planes associated with C-S fabrics in plutonic rocks are indicated.

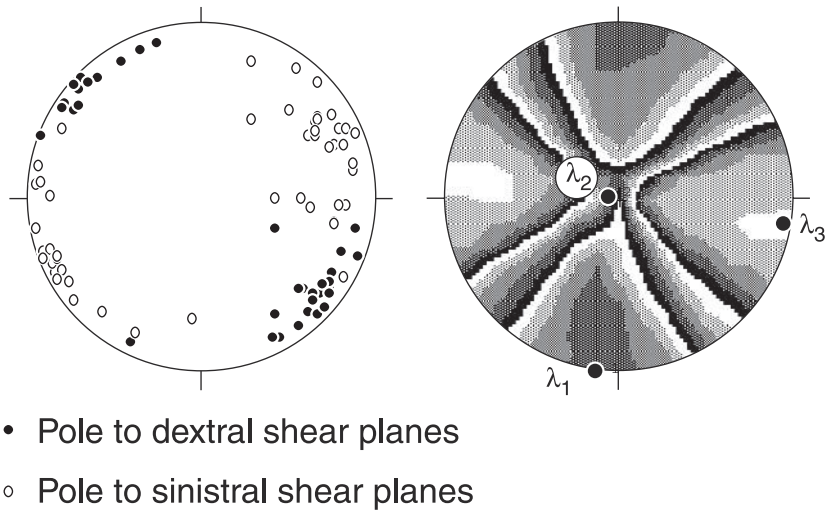

Figure 7. Stereograms showing the shear population measured for this study and the results of the statistical kinematic analysis with contours of λ_1 axes.

nattam pluton boundary-parallel shortening and E-W contraction (Figure 4) within a foliation triple point at the crest of the pluton [e.g., *Brun and Pons*, 1981].

[26] Relationships between the eastern granodiorite and western quartz-monzonite, on the one hand, and their country rocks (greenstones, gneiss, and migmatites), on the other hand, are similar to those between the Bisanattam pluton and the KGB. Indeed, the plutons' internal foliation parallels the country rocks' planar fabrics in the vicinity of their contact and pervasive C-S fabrics developed within the plutons. This suggests syntectonic emplacement during partitioned horizontal bulk inhomogeneous shortening, with preferential activation of the sinistral (eastern granodiorite) or dextral (western quartz-monzonite) set of shear surfaces during cooling against the greenstone belt.

[27] The Patna pluton is also interpreted as syntectonic with respect to E-W regional contraction and coeval with fabric development in the northern central KGB. This is supported by the parallelism between pluton foliations, planar fabrics inside the belt in the vicinity of the pluton's contact, and foliations within wall rocks along the western boundary of the pluton (Figure 3a). Map relations further suggest that the emplacement of the pluton postdates the development of the western mylonite zone and the LS tectonites in the western part of the central KGB south of Dodduru (Figures 2 and 3).

5. Interpretation, Structural Chronology, and U-Pb Dating

5.1. Structural Interpretation

[28] The structural analysis reveals the interference of three types of strain patterns. The first type of strain pattern is associated with the development of the western mylonite zone and the steep LS fabrics preserved in the western half of the central KGB. Kinematics of the mylonite zone suggest that this deformation event accommodated the sinking (i.e., sagduction) of the KGB as a result of the density contrast between granite-gneiss terrains and greenstones [e.g., *Bouhallier et al.*, 1993, 1995; *Chardon et al.*, 1996, 1998]. The second type of strain pattern resulted from E-W bulk inhomogeneous shortening of the KGB and its adjoining granite-gneiss terrains that produced the subvertical, N-S trending foliation and the pervasive conjugate strike-slip shear zone pattern. The occurrence of pervasive shallowly plunging lineations in the granite-gneiss terrains and the N-S elongate shape of the KGB attest to N-S horizontal stretching associated with E-W shortening. The third type of strain pattern developed as a result of syntectonic emplacement of the four plutons against and around the KGB. Pluton emplacement is at least partly coeval with E-W inhomogeneous shortening as the plutons developed N-S vertical foliation and dextral or sinistral C-S fabrics that are compatible with the regional conjugate shear zone pattern. This means that pluton emplacement has taken place during protracted regional inhomogeneous contraction. The fact that one of these syntectonic plutons, the Western quartz-monzonite, is affected by the western mylonite zone suggests that gravity-driven sagduction was at least partly coeval with regional contraction, although strike-slip shear bands are superimposed on the western mylonite zone in most places.

[29] Diapirism tent to produce downdip, steeply plunging lineations and regional contraction developed subhorizontal elongation. In addition, diapiric and contractional lineation patterns were perturbed by the interference between pluton expansion and regional shortening (subhorizontal lineations at the crest of the plutons and steep lineations on their sides) [*Brun and Pons*, 1981]. The combination of those three processes resulted in the complex lineation pattern seen in Figure 3b and the pitch transect shown in Figure 4. This is best expressed in the eastern part of the belt (in the vicinity of the eastern granodiorite and Bisanattam plutons). In contrast, the western half of the KGB preserved a pristine

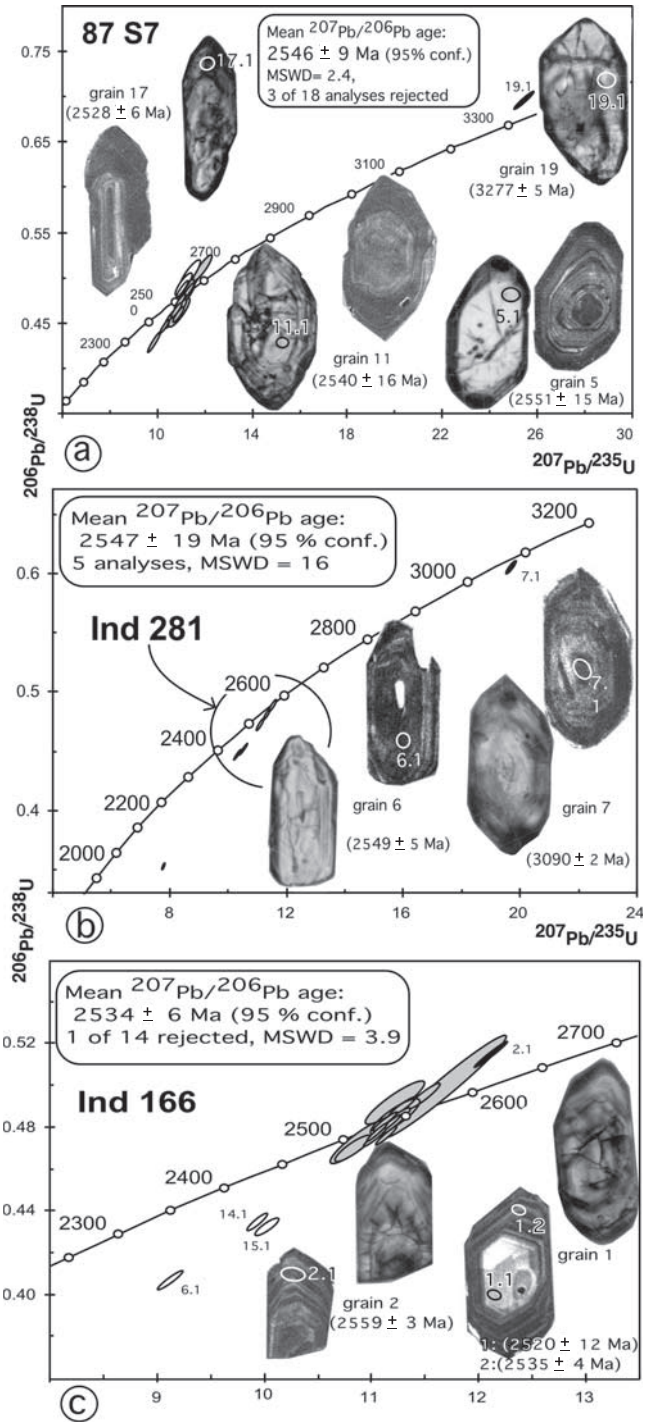

Figure 8. Zircon U-Pb concordia plots for samples (a) 87/S7, (b) IND 281, and (c) IND 166. See Table 1 for details.

diapiric lineation pattern, and the regional contractional lineation pattern is best seen outside the KGB (Figure 3c).

5.2. Constraints From SHRIMP U-Pb Geochronology

[30] The U-Pb ages of *Krogstad et al.* [1991] for the Dod (circa 2630 Ma) and Dossa (circa 2610 Ma) "gneisses" were obtained using the multigrain classical U-Pb dating method. The circa 2550 Ma sphene age of those samples is interpreted as a cooling age [*Krogstad et al.*, 1991]. The western quartz-monzonite has been dated in the south (sample 87/S7; Figure 2) at 2552 ± 2 Ma with some inheritance (>2800 Ma) by *Jayananda et al.* [2000] using the single-zircon evaporation method. As stated in section 3, our work suggests that the Dod and Dossa gneisses are part of the western quartz-monzonite (Figure 2). Furthermore, the crystallization age of the western quartz-monzonite should constrain the timing of E-W shortening and shearing in the western mylonite. Accordingly, we performed SHRIMP analyses of sample 87/S7 and a new sample (IND 281) from the northern part of the pluton (Figure 2).

[31] The 87/S7 sample (12°49′24″ E–78°14′30″N; Figure 2) is a strongly foliated facies of the western quartz-monzonite. In this sample, zircons are mainly of the S12/13 and S18/19 types of *Pupin* [1980] as classically found in calc-alkaline magmas. In transmitted light or Cl images, these zircons generally display a clearly zoned center surrounded by a thin, zoned rim that is generally enriched in U (Figure 8a and Table 1). There is no significant difference in age between the two zones, suggesting two steps in a magmatic evolution rather than inherited cores or magmatic overgrowths. Some clear and transparent grains with a fine magmatic zoning (grain 5; Figure 8a) have similar ages. Ages are subconcordant in the concordia diagram and define a $^{207}Pb/^{206}Pb$ average age of 2546 ± 9 Ma when the three circa 2.5 Ga youngest ages are rejected (grains 4, 15, 16) and 2542 ± 10 Ma on the 18 analyses. One grain, showing a lower Th/U ratio, has a larger development of 100 pyramide (S25-type?) (grain 19.1; Figure 8a) and is older with a $^{207}Pb/^{206}Pb$ age of 3277 ± 5 Ma. It is interpreted as an inherited xenocryst within a 2.54-Gyr-old magma.

[32] Sample IND 281 (12°59′28″E–78°12′41″N; Figure 2) is a strongly foliated porphyritic gneissic facies of the western quartz-monzonite from the western mylonite zone. On a limited number of analyses (five), it yields a $^{207}Pb/^{206}Pb$ average age of 2547 ± 19 Ma with an inherited xenocryst circa 3.09 Gyr old (Figure 8b and Table 1). This date and the one obtained for sample 87/S7 are similar and indicative of a magmatic event at circa 2.55 Ga, in agreement with the previous single grain evaporation dating of *Jayananda et al.* [2000]. Inheritance at circa 3.1 and 3.3 Ga is indicative of the ages of the surrounding gneisses as defined by *Krogstad et al.* [1991]. There is no evidence for a 2.6-Gyr-old magmatic event in our samples of the western quartz-monzonite. This suggests that the circa 2.6 Ga ages obtained by *Krogstad et al.* [1991] may result from the mixing of 2.55 Ga magmatic zircons with some ancient xenocrysts and that the sphene age at 2.55 Ga obtained by these authors is a magmatic age.

[33] Sample IND 166 of the Bisanattam pluton (12°51′74″E–44°16′34″N; Figure 2) is a C-S- fabrics-bearing trondhjemite. Its crystallization age should constrain the timing of E-W shortening and regional shearing. Zircons are of similar types to the ones previously described for sample 87/S7 (Figure 8c and Table 1) without any significant change in age between the central part of grains and the

Table 1. Summary of SHRIMP U-Pb Zircon Results[a]

Zircon Grain Spot	U, ppm	Th, ppm	Th/U	Pb*, ppm	$^{204}Pb/^{206}Pb$	f_{206}, %	Radiogenic Ratios						Ages, Ma				
							$^{206}Pb/^{238}U$	±	$^{207}Pb/^{235}U$	±	$^{207}Pb/^{206}Pb$	±	$^{206}Pb/^{238}U$	±	$^{207}Pb/^{206}Pb$	±	Conc., %
Sample 87/S7																	
1.1	620	436	0.70	215	0.000012	0.02	0.4798	0.0072	11.21	0.18	0.1694	0.0008	2526	31	2552	8	99
2.1	433	295	0.68	147	0.000101	0.14	0.4847	0.0083	11.30	0.21	0.1691	0.0010	2548	36	2549	9	100
3.1	132	126	0.96	42	0.000226	0.32	0.4557	0.0091	10.61	0.26	0.1688	0.0020	2421	40	2546	20	95
4.1	82	66	0.81	30	0.000304	0.42	0.5037	0.0129	11.37	0.35	0.1637	0.0023	2629	56	2494	24	105
5.1	222	275	1.24	79	0.000067	0.09	0.4817	0.0090	11.25	0.24	0.1693	0.0015	2535	39	2551	15	99
6.1	628	429	0.68	213	0.000066	0.09	0.4743	0.0071	10.96	0.18	0.1676	0.0010	2502	31	2534	10	99
7.1	669	462	0.69	219	0.000043	0.06	0.4593	0.0071	10.88	0.19	0.1719	0.0010	2436	32	2576	9	95
8.1	87	71	0.82	31	0.000111	0.16	0.4872	0.0171	11.24	0.42	0.1673	0.0018	2559	74	2530	18	101
9.1	592	548	0.93	204	0.000151	0.21	0.4638	0.0066	10.79	0.17	0.1687	0.0010	2456	29	2545	10	97
10.1	216	157	0.73	73	0.000050	0.07	0.4658	0.0087	10.95	0.24	0.1705	0.0015	2465	39	2563	15	96
11.1	221	178	0.81	80	0.000023	0.03	0.4927	0.0118	11.43	0.31	0.1682	0.0016	2582	51	2540	16	102
12.1	99	79	0.80	34	0.000010	0.01	0.4612	0.0133	10.91	0.36	0.1716	0.0023	2445	59	2574	23	95
13.1	136	96	0.71	47	0.000008	0.01	0.5112	0.0116	11.89	0.32	0.1686	0.0020	2662	50	2544	20	105
14.1	574	549	0.96	188	0.000143	0.20	0.4291	0.0087	9.87	0.21	0.1668	0.0009	2302	39	2526	10	91
15.1	164	129	0.79	59	0.000117	0.16	0.4928	0.0105	11.11	0.29	0.1635	0.0020	2583	46	2492	21	104
16.1	276	356	1.29	102	0.000065	0.09	0.4875	0.0072	11.04	0.18	0.1643	0.0010	2560	31	2500	10	102
17.1	645	634	0.98	202	0.000132	0.19	0.4466	0.0060	10.29	0.15	0.1670	0.0006	2380	27	2528	6	94
18.1	618	473	0.77	213	0.000064	0.09	0.4728	0.0067	11.09	0.17	0.1701	0.0006	2496	29	2559	6	98
19.1	611	51	0.08	290	0.000001	0.00	0.6959	0.0085	25.43	0.33	0.2650	0.0009	3405	33	3277	5	104
Sample IND 281																	
1.1	881	376	0.43	366	0.000030	0.04	0.4834	0.0033	11.319	0.084	0.1698	0.0005	2542	14	2556	5	99
2.1	735	210	0.29	285	0.000023	0.03	0.4502	0.0029	10.366	0.071	0.1670	0.0004	2396	13	2528	4	95
3.1	807	259	0.32	340	0.000001	0.00	0.4905	0.0031	11.532	0.076	0.1705	0.0003	2573	14	2563	3	100
4.1	926	431	0.47	362	0.000032	0.05	0.4544	0.0030	10.530	0.073	0.1681	0.0004	2415	13	2538	4	95
5.1	910	281	0.31	279	0.000063	0.09	0.3569	0.0021	7.773	0.050	0.1579	0.0004	1968	10	2434	4	81
6.1	351	171	0.49	143	0.000027	0.04	0.4745	0.0035	11.066	0.089	0.1691	0.0005	2503	15	2549	5	98
7.1	915	23	0.02	477	0.000032	0.04	0.6059	0.0036	19.680	0.121	0.2356	0.0003	3053	15	3090	2	99
Sample IND 166																	
1.1	75	31	0.41	30	0.000073	0.10	0.4728	0.0071	10.833	0.180	0.1662	0.0012	2496	31	2520	12	99
1.2	994	457	0.46	406	0.000001	<0.01	0.4749	0.0028	10.983	0.070	0.1677	0.0004	2505	12	2535	4	99
2.1	855	329	0.39	377	0.000020	0.03	0.5137	0.0043	12.054	0.103	0.1702	0.0003	2673	18	2559	3	104
3.1	1042	728	0.70	426	0.000039	0.05	0.4753	0.0028	11.078	0.068	0.1690	0.0003	2507	12	2548	3	98
4.1	151	91	0.60	63	–	<0.01	0.4813	0.0048	11.121	0.121	0.1676	0.0007	2533	21	2534	7	100
5.1	840	374	0.45	348	0.000005	0.01	0.4818	0.0029	11.073	0.071	0.1667	0.0004	2535	13	2525	4	100
6.1	724	448	0.62	254	0.000121	0.17	0.4075	0.0031	9.071	0.074	0.1615	0.0004	2203	14	2471	4	89
7.1	439	337	0.77	185	0.000013	0.02	0.4890	0.0032	11.233	0.079	0.1666	0.0004	2567	14	2524	4	102
8.1	55	16	0.29	23	0.000000	<0.01	0.4842	0.0056	11.157	0.150	0.1671	0.0012	2546	24	2529	12	101
9.1	281	116	0.41	120	0.000127	0.18	0.4943	0.0041	11.436	0.102	0.1678	0.0006	2589	18	2536	6	102
9.2	138	58	0.42	59	0.000039	0.05	0.4983	0.0157	11.616	0.376	0.1691	0.0013	2607	67	2548	13	102
10.1	739	253	0.34	305	0.000001	<0.01	0.4811	0.0030	11.112	0.073	0.1675	0.0003	2532	13	2533	3	100
11.1	173	109	0.63	70	0.000092	0.13	0.4689	0.0041	10.790	0.109	0.1669	0.0008	2479	18	2527	8	98
12.1	106	49	0.46	45	0.000206	0.29	0.4911	0.0069	11.161	0.178	0.1648	0.0012	2575	30	2506	12	103
13.1	726	650	0.90	297	0.000015	0.02	0.4771	0.0029	11.003	0.071	0.1673	0.0003	2515	13	2530	3	99
14.1	992	1046	1.05	372	0.000165	0.23	0.4348	0.0026	9.872	0.062	0.1647	0.0003	2327	12	2504	3	93
15.1	518	421	0.81	193	0.000322	0.45	0.4328	0.0027	9.977	0.076	0.1672	0.0007	2318	12	2530	7	92

[a] Uncertainties are given at the 1σ level. The f_{206} percentage denotes the percentage of ^{206}Pb that is common Pb. Correction for common Pb is made using the measured $^{204}Pb/^{206}Pb$ ratio. A concentration percentage of 100% denotes a concordant analysis.

zoned rims (grain 1, for example). A mean $^{207}Pb/^{206}Pb$ age at 2534 ± 6 Ma is defined, this age being similar to that obtained by *Krogstad et al.* [1991] for the eastern granodiorite (2532 ± 3 Ma).

[34] These results, together with the ages reported by *Krogstad et al.* [1991], indicate that the four syntectonic plutons (Patna, Bisanattam, eastern granodiorite, and western quartz-monzonite) were emplaced during a relatively short period of time (2552–2532 Ma) and that the regional shear zone pattern developed during this time interval. The age obtained on the western quartz-monzonite within the mylonite zone (IND 281) further shows that downward displacement of the greenstones along the western décollement was active at least after 2547 ± 19 Ma. The 2552 Ma U-Pb age of the Patna pluton [*Krogstad et al.*, 1991] is consistent with this result as the emplacement of this pluton partly postdates the western mylonite (Figure 2).

6. Regional Structural Analysis

[35] West of the western quartz-monzonite (Figure 9), the dominant rock types are gray gneisses and migmatites

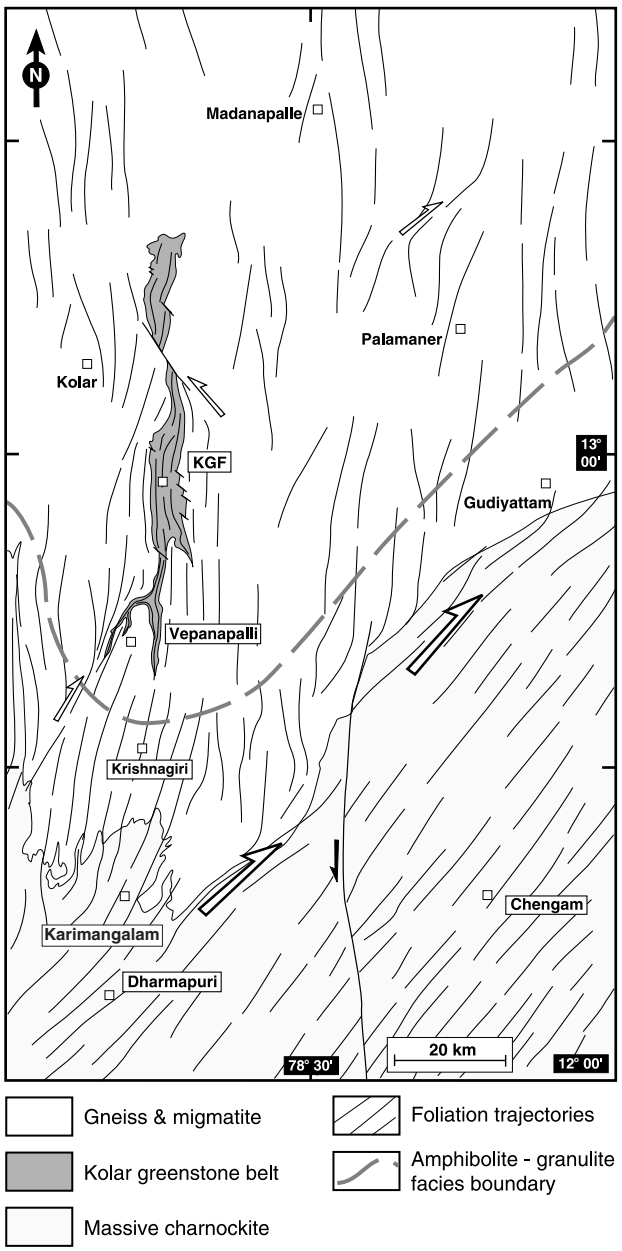

Figure 9. Regional structural map showing the relations between the Kolar greenstone belt and the amphibolite-granulite transition zone. Sources for the data are the *Geological Survey of India* [1994a, 1994b] and the present work. For location, see Figure 1.

intruded by some 2540-Myr-old plutons [*Jayananda et al.*, 2000]. East of the eastern granodiorite, the migmatites grade into leucocratic to light grayish diatexites and few minor plutons (Figure 9) displaying the same structural pattern as the one affecting the basement rocks around the KGB (pervasive steep, N-S trending foliations, subhorizontal lineations and conjugate shear zone pattern), but the degree of melting is higher than around the greenstone belt. Field relations show that melting was synkinematic with respect to shearing as attested to by the pervasive occurrence of melt-filled shear zones.

[36] From the KGB to Salem (Figures 1 and 9) a pristine unbroken section toward lower crustal levels across the amphibolite-granulite transition is exposed [*Condie et al.*, 1982; *Hansen et al.*, 1995]. Paleodepths of 14 and 28 km are recorded in Krishnagiri and Salem, respectively, with a corresponding synmetamorphic paleotemperature increase from 650° to 800°C [*Hansen et al.*, 1995]. South of the amphibolite-granulite facies boundary, the regional foliation is deflected into NE orientation toward the south in the vicinity of the charnockitic front (Figure 9). This map pattern together with our field observations indicate a regional strain gradient into a major dextral shear zone that coincides with a shear belt interpreted from LANDSAT images by *Drury and Holt* [1980]. The results of our detailed structural analysis within a corridor going from

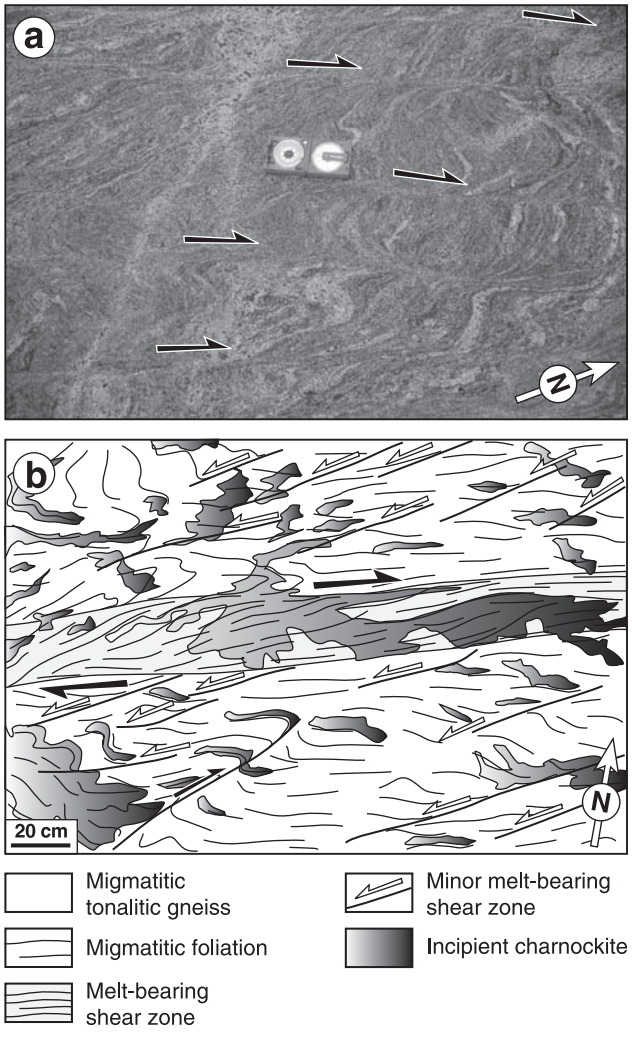

Figure 10. (a) Synmigmatitic dextral shear bands in the juvenile tonalitic gneisses 6.5 km E of Krishnagiri (Figure 9). (b) Relations between synmigmatitic shear zones and incipient charnockites (9 km NW of Karimangalam; Figure 9).

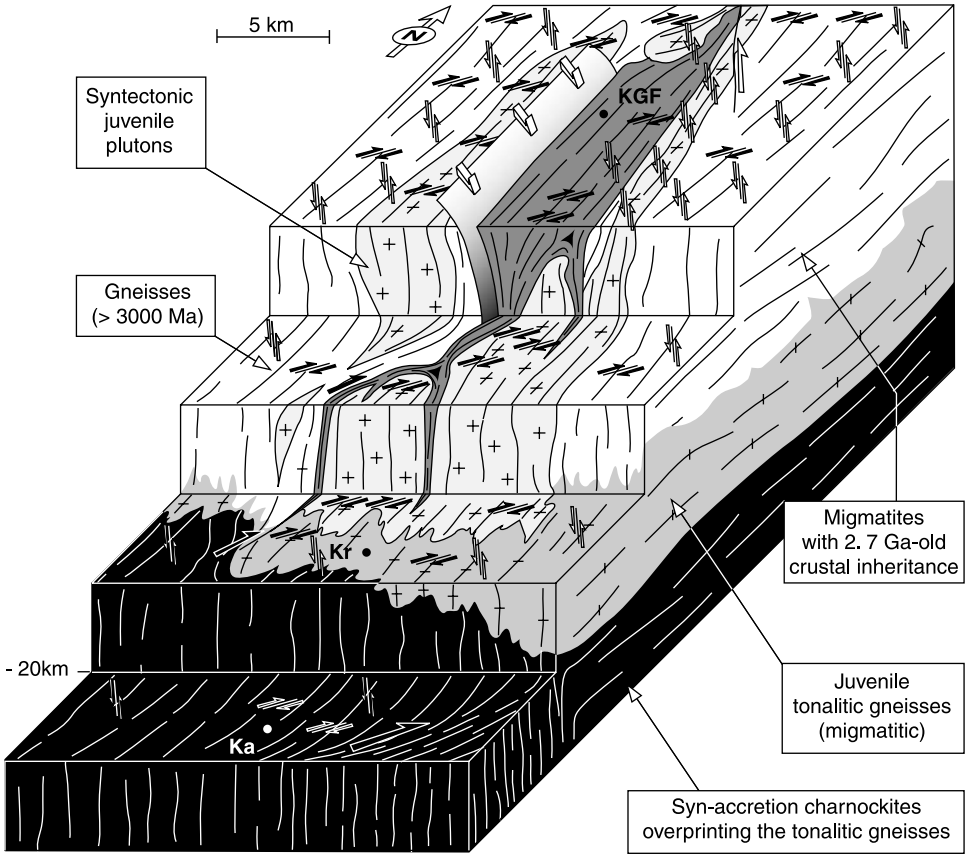

Figure 11. Sketch summarizing the three-dimensional crustal-scale strain pattern and the kinematics of the Kolar Gold Fields (KGF), Krishnagiri (Kr), and Karimangalam (Ka) area.

Vepanapalli (southern KGB) to Karimangalam (Figure 9) are summarized as follows.

[37] A N-S elongate pluton that shares many petrographical and structural similarities with the Bisanattam pluton cores the Vepanapalli antiform and intrudes the KGB. It is homogeneous, with a steep N-S striking foliation and pervasive, NE to NNE trending dextral C-S fabrics. Late ductile to brittle-ductile conjugate sinistral shear bands are locally superimposed on the dextral C-S fabrics. Toward the south around Krishnagiri, the plutons are replaced by migmatitic tonalitic gneisses that are affected by pervasive dextral shear bands trending N20° to N40° collecting the melts (Figure 10a), and late-melt to postmelt conjugate sinistral shear bands. These structural features are preserved south of the granulite facies isograd where NE striking decimeter to millimeter thick dextral shear zones are filled with synkinematic diatexitic melts (Figure 10b). These shear zones overprint conjugate sets of strike-slip shear bands that are deflected into the shear zones. Orthopyroxene-bearing charnockitic patches (i.e., incipient charnockites) preferentially affect the leucosomes and the diatexites and have mutually crosscutting relationships with the shear zones (Figure 10b). This, together with the fact that the shear zones are coeval with melting, indicates that the finite structural pattern was produced by ongoing shearing during melting and high-grade metamorphism. Farther south, toward Dharmapuri, the planar fabrics are deflected into the regional-scale shear zone, kinematically compatible with the dextral shear zones developed from the charnockitic front. Those relations are summarized in Figure 11.

[38] The migmatitic tonalitic gneisses of the transition zone are juvenile and were emplaced at 2550–2530 ± 5 Ma [*Peucat et al.*, 1989, 1993a]. The massive charnockites and the tonalitic gneisses went through the U-Pb monazite closure temperature (~700°C) at 2506 ± 10 and 2517 ± 10 Ma, respectively [*Peucat et al.*, 1993a], suggesting cooling from peak granulite facies metamorphic conditions.

7. Interpretation and Discussion

7.1. Development of the Three-Dimensional Tectonomagmatic Pattern

[39] A juvenile TTG magmatic complex, resulting from melting of underplated metabasalts, was emplaced between 2550 and 2530 Ma in the Kolar-Krishnagiri crustal panel. At high structural levels, around the KGB, the juvenile melts formed syntectonic plutons (Figure 11). The deep part of this accreted complex (i.e., tonalitic gneisses) underwent subsequent melting and charnockitization slightly after its emplacement (after 2530 Ma, the youngest zircon U-Pb age of those melts, and before 2517 Ma, their Monazite U-Pb

age). This magmatic complex and its country rocks display the same tectonic fabrics (N-S trending, steep foliation, shallowly plunging lineation, and conjugate strike-slip shear zone pattern; Figure 11). The continuity and compatibility of this synmelt and synmetamorphic structural pattern from middle to lower crustal levels further indicate that bulk inhomogeneous contraction, metamorphism, melting, and plutonism were synchronous throughout the crust. This regional deformation event was coeval with or postdated diapirism between the greenstone belt and the surrounding rocks. The western mylonite zone is probably a sheared unconformity between a greenstone basin and a >3000-Myr-old basement similar to the gravity-driven décollement layers mapped at the base of the Dharwar Supergroup [*Chardon et al.*, 1996, 1998].

[40] Regional inhomogeneous shortening produced moderate strain of the crustal panel that was bounded to the southeast by an active NE trending dextral shear zone. Indeed, dextral shear bands associated with this shear zone are coeval with granulite facies metamorphism and the development of the charnockites that cooled under 700°C around 2520 Ma. These results suggest that this regional shear zone is not Proterozoic as suggested by *Drury and Holt* [1980] and *Drury et al.*, [1984] but mainly late Archean in age and developed during regional metamorphism and deformation at 2550–2530 Ma. Our interpretation does not preclude local reactivation of the core of this shear zone as attested to by the emplacement of Late Proterozoic syenite and carbonatite bodies [e.g., *Anil Kumar et al.*, 1998; *Miyazaki et al.*, 2000].

7.2. Test of the Cordilleran Tectonic Model

[41] *Krogstad et al.* [1989] have compared the southeastern Dharwar craton with the Mesozoic northwestern American active margin. They have proposed that between 2530 Ma and 2420 Ma (Ar-Ar age) the KGB had been the locus of the amalgamation of two contrasted continental crustal segments (i.e., a western block with a 3100–3300-Myr-old continental component and an eastern, 2.5-Gyr-old juvenile island arc). For those authors, this collage would have been accommodated by a N-S striking shear zone coinciding with the KGB in a context of left-oblique convergence. The present work shows that deformation ended by 2530 Ma instead of 2420 Ma and recently acquired geochronological data (J. J. Peucat et al., in preparation) show that continental basement at least 2.7-Gyr-old is, in fact, present east of the KGB.

[42] The geometry of the pervasive conjugate strike-slip shear zone pattern and the systematic obliquity between the granite-greenstone contact and the great axis of the belt, on one hand, and the shear planes, on the other hand (Figure 6), indicate that the elongated shape of the KGB parallels the regional N-S finite elongation direction instead of a shearing direction. Indeed, shearing directions are either NW (sinistral set) or NE (dextral set) striking, whereas the greenstone belt is N-S striking. Furthermore, the western boundary of the belt is a gravity-driven décollement associated with dip-slip shearing and not a strike-slip shear zone. Therefore horizontal displacement across the greenstone belt was limited during the main and last deformation episode. Pervasive regional deformation is characterized by E-W bulk inhomogeneous shortening accommodated by a conjugate strike-slip shear zone network, a N-S trending vertical foliation, and a subhorizontal N-S trending stretching lineation in basement rocks. Displacement along both sets of shear zones is limited, as they do not disrupt the KGB at the scale of the study area (Figure 6). This suggests that the 2550–2530 Ma episode resulted in horizontal plane strain (i.e., no shortening or thickening along the λ_2 vertical axis, a horizontal N-S trending λ_1 stretching axis, and a horizontal E-W trending λ_3 shortening axis) and pure shear (nonrotational coaxial deformation). The 2550–2530 Ma deformation episode characterized here is associated with the emplacement of juvenile plutons and reworking of preexisting crust on both sides of the KGB. It also produced a similar strain pattern on both sides of the belt and the same strike-slip shear zone network within and outside the KGB. To our view, only a previously coherent crustal panel containing the KGB could develop such a symmetrical and distributed strain pattern.

[43] Oblique and even straight-on convergence is accommodated at Phanerozoic active plate margins by strike-slip partitioning of transpressional deformation [*Teyssier et al.*, 1995]. Large-scale strike-slip simple shear zones develop parallel to the plate boundary, especially in magmatic arcs [e.g., *Saint Blanquat et al.*, 1998; *Chardon et al.*, 1999; *Chardon*, 2002], leading to strain localization and asymmetrical strain patterns [*Choukroune et al.*, 1987]. Furthermore, in transpressional contexts, steep to vertical lineations and thrust fabrics develop to accommodate the contractional component of deformation, and produce crustal thickening. The symmetrical structural pattern and geochronological data described here for the KGB and surrounding crust is not compatible with such modern transpressive structural patterns.

[44] The largest magmatic arc of the North American Cordillera (the Coast Plutonic Complex) was built by accretion of thin (5 to 20 km thick) elongate (up to hundreds of kilometers long) plutonic belts of distinct ages [*van der Heyden*, 1992]. The emplacement of those belts was controlled by strike-slip partitioned transpression along large-scale shear zones during oblique plate convergence over long time periods (50 to 150 Myr) and was coeval with the development of thrust belts displaying reverse metamorphic gradients [e.g., *Chardon et al.*, 1999]. The southeastern Dharwar craton underwent an accretion super event during a short time period (2550–2530 Ma) and over a very wide area (>60,000 km^2) [*Jayananda et al.*, 2000] that was undergoing distributed pure shear deformation and limited crustal thickening. It is also worth noting that the systematic isobaric cooling paths recorded by the late Archean granulites of the craton [*Raith et al.*, 1983] support the idea that the region had not undergone significant thickening during the tectonic event that lead to granulite metamorphism [e.g., *Sandiford*, 1989].

[45] To summarize, the tectonoplutonic pattern described here is significantly different from the one developed along

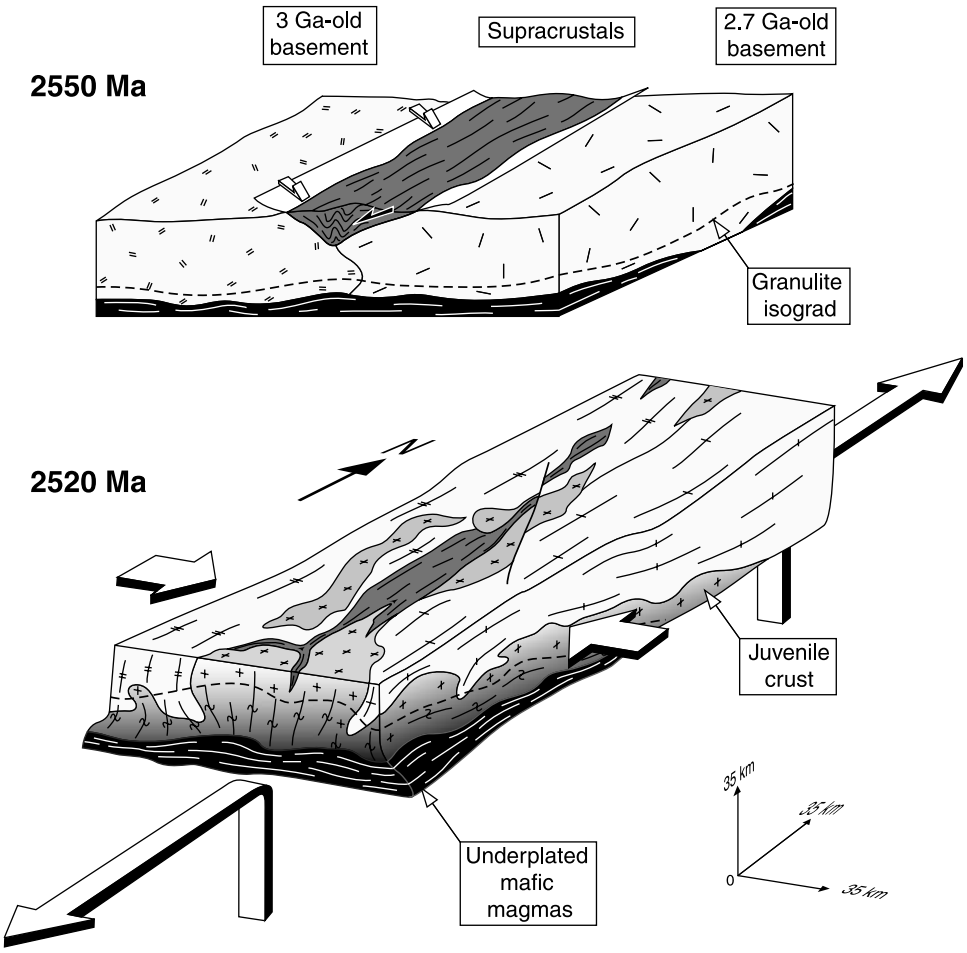

Figure 12. Block diagrams representing two stages in the evolution of the southeastern Dharwar craton during the late Archean magmatic accretion event. See text for comments.

Phanerozoic convergent plate boundary as exemplified by the Coast Plutonic Complex. We conclude that deformation of the Kolar granite-greenstone terrain was produced between 2550 and 2530 Ma and that this deformation did not accommodate oblique convergence nor terrain amalgamation. The style and extent of the 2550–2530 Ma episode in the southeastern Dharwar craton rather suggest interplay of diapirism, regional inhomogeneous contraction, and voluminous lower crustal and midcrustal juvenile magmatic accretion throughout a crustal panel containing the previously assembled KGB and 3.3 to 2.7-Gyr-old basement gneiss segments (Figure 12). The model proposed by *Krogstad et al.* [1989] might still apply to the KGB area but before 2550 Ma although the crust to the east of the KGB is not entirely juvenile as it contains relics of 2.7-Gyr-old crust. The deformation pattern that presided at the earlier magmatic and/or tectonic juxtaposition of the two contrasting continental segments from both sides of the KGB would have been erased by the 2550–2530-Myr-old intracontinental tectonic strain fabrics. Lateral accretion (between 2.7 and 2.55 Ga) followed by intracontinental reworking during juvenile underaccretion is rather compatible with the geodynamic model of *Choukroune et al.* [1997].

7.3. A Specific Archean Synaccretion Tectonic Process

[46] The Kolar-Krishnagiri regional strain pattern requires a specific crustal rheological structure to develop. Indeed, this structure implies low mechanical contrast in the middle-lower crust (i.e., mechanical homogeneity provided by temperature buffering throughout the middle lower crust), and a low viscosity that did not allow the crust to sustain thickening. Such conditions are fulfilled thanks to the steep advective geotherm provided by magmatic underaccretion leading to pervasive regional melting in the middle and lower crust. The fact that the greenstones have sunk into the crust also suggests these specific rheological conditions [*Chardon et al.*, 1998; *Mège et al.*, 2000]. Regional horizontal pure shear further requires specific boundary conditions to develop. Indeed, the northern and/or southern edges of the deforming system must have acted as a free mechanical boundary allowing N-S horizontal flow to compensate E-W shortening. As the Kolar-Krishnagiri

structural pattern appears to develop within a crustal panel that was bounded to the SE by an active NE trending dextral shear zone, such a free boundary may have to be found in the northern part of the craton. The Kolar crustal panel may also be bounded to the west and to the north by some regional anastomosed shear zones (NNW trending sinistral and NE trending dextral) similar to the ones developed in the western Dharwar craton [e.g., *Bouhallier et al.*, 1995]. In that case, the Kolar panel would represent a low strain domain (a tectonic lens) within the regional conjugate shear zone network [*Gapais et al.*, 1987].

[47] The development of a huge thermal anomaly associated with regional juvenile magmatic underaccretion allowed gravity tectonics and distributed horizontal pure shear deformation to take place in the southeastern Dharwar craton at 2.5 Ga. As stated in section 7.2, there are marked differences between the Kolar tectonomagmatic pattern and modern active plate margins. Furthermore, the size of this short-lived thermal instability seems difficult to reconcile with today's magmatic arcs thermal regimes. Indeed, the temperature anomaly is highly anisotropic and parallel to the plate margin in Phanerozoic Cordilleran orogens, leading to long-lived magmatic and metamorphic breaks normal to the orogen-parallel regional structural grain. In the southern Dharwar craton, regional metamorphic isograds are subhorizontal and normal to the N-S structural trend (Figure 1). For these reasons, we suggest that the 2.5 Ga event in South India is better explained by the interaction of this continental crustal segment with a mantle plume during regional contraction (Figure 12). As regional contraction and plume activity were coeval, the horizontal spreading component of deformation due to plume effect was forced perpendicular to the regional shortening direction (Figure 12) and accommodated by spreading at a free mechanical boundary [e.g., *Bailey*, 1999]. This allowed regional-scale nonisovolumetric, horizontal, plane strain pure shear deformation enabling significant addition of juvenile material to the crust without tectonic crustal thickening.

8. Conclusions

[48] The Kolar granite-greenstone pattern was produced by the interference of gravity-driven sagging of the greenstones (diapirism) and bulk inhomogeneous regional E-W shortening combined with horizontal N-S stretching during juvenile magmatic underaccretion and granulite metamorphism between 2550 and 2530 Ma. This accretion event took place in an intracontinental setting and contributed to crustal growth without significantly thicken the crust, thanks to a specific structural process involving regionally distributed, horizontal pure shear deformation. Such structural process does not operate in Phanerozoic magmatic arcs and may require mantle plume activity at the base of the crust to produce large-scale magmatic underaccretion, thermal buffering and lateral spreading of the crust.

[49] **Acknowledgments.** This work was funded by the Indo-French Center for the Promotion of Advanced Research (project 2307-1). Fieldwork for M. J. was partially supported by Government of India DST project grant ESS/16/077/96. We acknowledge the Isis program that provided the SPOT satellite images (copyright CNES). We thank B. Mahabaleswar for support, V. N. Vasudev for discussions in the field, R. Capdevila for petrological determinations, and D. Gapais for comments and suggestions on an early draft of the manuscript. A thorough review by an anonymous referee and comments by F. Schwerdtner helped us to improve the paper.

References

Anil Kumar, S. N. Charan, K. Gopalan, and J. D. MacDougall, A long-lived enriched mantle source for two Proterozoic carbonatite complexes from Tamil Nadu, southern India, *Geochim. Cosmochim. Acta*, *62*, 515–523, 1998.

Bailey, R. C., Gravity-driven continental overflow and Archaean tectonics, *Nature*, *398*, 413–415, 1999.

Balakrishnan, S., and V. Rajamani, Geochemistry and petrogenesis of granitoids around the Kolar Schist Belt, south India: Constraints for the evolution of the crust of the Kolar area, *J. Geol.*, *95*, 219–240, 1987.

Balakrishnan, S., G. N. Hanson, and V. Rajamani, Pb and Nd isotope constraints on the origin of high Mg and tholeitic amphibolites, Kolar schist belt, South India, *Contrib. Mineral. Petrol.*, *107*, 279–292, 1990.

Balakrishnan, S., V. Rajamani, and G. N. Hanson, U-Pb ages of zircon and titanite from the Ramagiri area, Southern India: Evidence for accretionary origin of the Eastern Dharwar craton during the Late Archaean, *J. Geol.*, *107*, 69–86, 1999.

Berthé, D., P. Choukroune, and P. Jégouzo, Orthogneiss, mylonite and non coaxial deformation of granites: The example of the South Armorican Shear Zone, *J. Struct. Geol.*, *1*, 31–42, 1979.

Bouhallier, H., Evolution structurale et métamorphique de la croûte continentale Archéenne (Craton de Dharwar, Inde du Sud), *Mém. Géosci. Rennes*, *60*, 1995.

Bouhallier, H., P. Choukroune, and M. Ballèvre, Diapirism, bulk homogeneous shortening and transcurrent shearing in the Archaean Dharwar craton: The Holenarsipur area, southern India, *Precambrian Res.*, *63*, 43–58, 1993.

Bouhallier, H., D. Chardon, and P. Choukroune, Strain patterns in Archaean dome-and-basin structures: The Dharwar craton (Karnataka, South India), *Earth Planet. Sci. Lett.*, *135*, 57–75, 1995.

Brun, J.-P., and J. Pons, Strain patterns of pluton emplacement in a crust undergoing non-coaxial deformation, Sierra Morena, Southern Spain, *J. Struct. Geol.*, *3*, 219–229, 1981.

Chadwick, B., V. N. Vasudev, and G. V. Hedge, The Dharwar craton, southern India, interpreted as the result of Late Archaean oblique convergence, *Precambrian Res.*, *99*, 91–101, 2000.

Chardon, D., Les déformations continentales archéennes: Exemples naturels et modélisation thermomécanique, *Mém. Géosci. Rennes*, *76*, 1997.

Chardon, D., Strain partitioning and batholith emplacement at the root of a transpressive magmatic arc, *J. Struct. Geol.*, in press, 2002.

Chardon, D., P. Choukroune, and M. Jayananda, Strain patterns, décollement and incipient sagducted greenstone terrains in the Archaean Dharwar craton (South India), *J. Struct. Geol.*, *18*, 991–1004, 1996.

Chardon, D., P. Choukroune, and M. Jayananda, Sinking of the Dharwar basin (South India): Implications for Archaean tectonics, *Precambrian Res.*, *91*, 15–39, 1998.

Chardon, D., C. L. Andronicos, and L. S. Hollister, Large scale transpressive shear zone patterns and displacements within magmatic arcs: The Coast Plutonic Complex, British Columbia, *Tectonics*, *18*, 278–292, 1999.

Choukroune, P., D. Gapais, and O. Merle, Shear criteria and structural symmetry, *J. Struct. Geol.*, *9*, 525–530, 1987.

Choukroune, P., H. Bouhallier, and N. T. Arndt, Soft lithosphere during periods of Archean crustal growth or crustal reworking, in *Early Precambrian Processes*, edited by M. P. Coward and A. C. Ries, *Geol. Soc. Spec. Publ. 95*, 67–86, 1995.

Choukroune, P., J. N. Ludden, D. Chardon, A. J. Calvert, H. Bouhallier, Archaean crustal growth and tectonic processes: A comparison of the Superior Province, Canada and the Dharwar craton, India, in *Orogeny Through Time*, edited by J.-P. Burg and M. Ford, *Geol. Soc. Spec. Publ.*, *121*, 63–98, 1997.

Collins, W. J., M. J. Van Kranendonk, and C. Teyssier, Partial convective overturn of Archaean crust in the East Pilbara craton, Western Australia: Driving mechanisms and tectonic implications, *J. Struct. Geol.*, *20*, 1405–1424, 1998.

Condie, K. C., P. Allen, and B. L. Narayana, Geochemistry of the Archean low- to high-grade transition zone, southern India, *Contrib. Mineral. Petrol.*, *81*, 157–167, 1982.

Drury, S. A., and R. W. Holt, The tectonic framework of the South Indian craton: A reconnaissance involving LANDSAT imagery, *Tectonophysics*, *65*, T1–T15, 1980.

Drury, S. A., N. B. Harris, R. W. Holt, G. J. Reeves-Smith, and R. T. Wightman, Precambrian tectonics and crustal evolution in South India, *J. Geol.*, *92*, 3–20, 1984.

Friend, C. R. L., and A. P. Nutman, SHRIMP U-Pb geochronology of the Closepet granite and Peninsular gneisses, Karnataka, South of India, *J. Geol. Soc. India*, *38*, 357–368, 1991.

Gapais, D., Shear structures within deformed granites: Thermal and mechanical indicators, *Geology*, *17*, 1144–1147, 1989.

Gapais, D., P. Balé, P. Choukroune, P. Cobbold, Y. Mahjoub, and D. Marquer, Bulk kinematics from shear zone patterns: Some field examples, *J. Struct. Geol.*, *9*, 635–646, 1987.

Geological Survey of India, Quadrangle map 57K, scale 1:250,000, Bangalore, 1994a.

Geological Survey of India, Quadrangle map 57L, scale 1:250,000, Bangalore, 1994b.

Ghosh, S. K., and S. Sengupta, Superimposed folding and shearing in the western quartzite of the Kolar gold field, *Indian J. Earth Sci.*, *12*, 63–67, 1985.

Hamilton, J. V., and C. J. Hodgson, Mineralization and structure of the Kolar gold field, India, paper presented at Gold '86 Symposium, Konsult Int., Toronto, 1986.

Hansen, E. C., R. C. Newton, A. S. Janardhan, and S. Lindenberg, Differentiation of Late Archean crust in the Eastern Dharwar craton, Krishnagiri-Salem area, South India, *J. Geol.*, *103*, 629–651, 1995.

Jayananda, M., H. Martin, J.-J. Peucat, and B. Mahabaleswar, Late Archaean crust-mantle interactions: Geochemistry of LREE-enriched mantle derived magmas: Example of the Closepet batholith, Southern India, *Contrib. Mineral. Petrol.*, *119*, 314–329, 1995.

Jayananda, M., J.-F. Moyen, H. Martin, J.-J. Peucat, B. Auvray, and B. Mahabaleswar, Late Archaean (2550-2520 Ma) juvenile magmatism in the Eastern Dharwar craton, southern India: Constraints from geochronology, Nd-Sr isotopes and whole rock geochemistry, *Precambrian Res.*, *99*, 225–254, 2000.

Jelsma, H. A., P. A. Van Der Beek, and M. L. Vinyu, Tectonic evolution of the Bindura-Shamva greenstone belt (northern Zimbabwe): Progressive deformation around diapiric batholiths, *J. Struct. Geol.*, *15*, 163–176, 1993.

Krogstad, E. J., S. Balakrishnan, D. K. Mukhopadhyay, V. Rajamani, and G. N. Hanson, Plate tectonics 2.5 billion years ago: Evidence at Kolar, South India, *Science*, *243*, 1337–1340, 1989.

Krogstad, E. J., G. N. Hanson, and V. Rajamani, U-Pb ages of zircon and sphene for two gneiss terranes adjacent to the Kolar schist belt, South India: Evidence for separate crustal evolution histories, *J. Geol.*, *99*, 801–816, 1991.

Krogstad, E. J., G. N. Hanson, and V. Rajamani, Sources of continental magmatism adjacent to the Late Archean Kolar suture zone, south India: Distinct isotopic and elemental signatures of two Late Archean magmatic series, *Contrib. Mineral. Petrol.*, *122*, 159–173, 1995.

Martin, H., The Archean grey gneisses and the genesis of the continental crust, in *Archean Crustal Evolution*, edited by K. C. Condie, pp. 205–259, Elsevier Sci., New York, 1994.

Mège, D., D. Chardon, and V. L. Hansen, Rayleigh-Taylor instability-driven plume tectonics and the rheology of the Archean, Venusian and Martian crusts, *Lunar Planet. Sci.* [CD-ROM], *XXXI*, 2000.

Miyazaki, T., H. Kagami, K. Shuto, T. Morikiyo, V. Ram Mohan, and K. C. Rajasekaran, Rb-Sr geochronology, Nd-Sr isotopes and whole rock geochemistry of Yelagiri and Sevattur syenites, Tamil Nadu, South India, *Gondwana Res.*, *3*, 39–53, 2000.

Moyen, J.-F., H. Martin, and M. Jayananda, Multi-element geochemical modeling of crust-mantle interactions during late-Archaean crustal growth: The Closepet granite (South India), *Precambrian Res.*, *112*, 87–105, 2001.

Mukhopadhyay, D. K., Significance of small-scale structures in the Kolar schist belt, South India, *J. Geol. Soc. India*, *33*, 291–308, 1989.

Mukhopadhyay, D. K., Deformational history of the Precambrian Kolar schist belt, South India: Constraints for the tectonic evolution, *Proc. Indian Acad. Sci. Earth Planet. Sci.*, *99*, 201–213, 1990.

Mukhopadhyay, D. K., and B. W. Haimanot, Geometric analysis and significance of mesoscopic shear zones in the Precambrian gneisses around the Kolar schist belt, South India, *J. Struct. Geol.*, *11*, 569–581, 1989.

Newton, R. C., The late Archean high-grade terrain of South India and the deep structure of the Dharwar craton, in *Exposed Cross–Sections of the Continental Crust*, edited by M. H. Salisbury and D. M. Fountain, pp. 305–326, Kluwer Acad., Norwell, Mass., 1990.

Nutman, A. P., B. Chadwick, B. Krishna Rao, and V. N. Vasudev, SHRIMP U-Pb zircon ages of acid volcanic rocks in the Chitradurga and Sandur Groups, and granites adjacent to the Sandur schist belt, Karnataka, *J. Geol. Soc. India*, *47*, 153–164, 1996.

Peucat, J.-J., P. Vidal, J. Bernard-Griffiths, and K. C. Condie, Sr, Nd and Pb isotopic systematics in the Archaean low- to high-grade transition zone of southern India: Syn-accretion vs. post-accretion granulites, *J. Geol.*, *97*, 537–550, 1989.

Peucat, J. J., B. Mahabaleswar, and M. Jayananda, Age of younger tonalitic magmatism and granulitic metamorphism in the South Indian transition zone (Krishnagiri area): Comparison with older Peninsular gneisses from the Gorur-Hassan area, *J. Metamorph. Geol.*, *11*, 879–888, 1993a.

Peucat, J.-J., G. Gruau, H. Martin, B. Auvray, S. Fourcade, P. Choukroune, H. Bouhallier, and M. Jayananda, A 2.5 Ga megaplume in South India?, *Terra Nova*, *97*, 321, 1993b.

Peucat, J. J., H. Bouhallier, C. M. Fanning, and M. Jayananda, Age of the Holenarsipur greenstone belt, relationships with the surrounding gneisses (Karnataka, South India), *J. Geol.*, *103*, 701–710, 1995.

Pupin, J.-P., Zircon and granite petrology, *Contrib. Mineral. Petrol.*, *73*, 207–220, 1980.

Raase, P., M. Raith, D. Ackermand, and R. K. Lal, Progressive metamorphism of mafic rocks from greenschist to granulite facies in the Dharwar Craton of south India, *J. Geol.*, *94*, 261–282, 1986.

Raith, M., P. Raase, D. Ackermand, and R. K. Lal, Regional geothermobarometry in the granulite facies terrane of South India, *Trans. R. Soc. Edinburgh Earth Sci.*, *73*, 221–244, 1983.

Rajamani, V., E. Krogstad, S. Balakrishnan, and G. Hanson, Are the Patna and Bisanattam granites (adjoining the Kolar schist belt) cogenetic?, *J. Geol. Soc. India*, *30*, 98–105, 1987.

Saint Blanquat (de), M., B. Tikoff, C. Teyssier, and J.-L. Vigneresse, Transpressional kinematics and magmatic arcs, in Continental Transpressional and Transtensional Tectonics, edited by R. E. Holdsworth, R. A. Strachan, and J. F. Dewey, *Geol. Soc. Spec. Publ. 135*, 327–340, 1998.

Sandiford, M., Horizontal structures in granulite terrains: A record of mountain building or mountain collapse?, *Geology*, *17*, 449–452, 1989.

Swami Nath, J., and M. Ramakrishnan, Present classification and correlation, in *Early Precambrian Supracrustals of Southern Karnataka*, edited by J. Swami Nath and M. Ramakrishnan, *Mem. Geol. Surv. India*, *112*, 23–38, 1981.

Swami Nath, J., M. Ramakrishnan, and M. N. Viswanatha, Dharwar stratigraphic model and Karnataka craton evolution, *Rec. Geol. Surv. India*, *107*, 149–175, 1976.

Teyssier, C., B. Tikoff, and M. Markley, Oblique plate motion and continental tectonics, *Geology*, *23*, 447–450, 1995.

Trendall, A. F., J. R. de Laeter, D. R. Nelson, and D. Mukhopadhyay, A precise U-Pb age for the base of the BIF of the Mulaingiri formation (Bababudan Group, Dharwar Supergroup) of the Karnataka craton, *J. Geol. Soc. India*, *50*, 161–170, 1997.

Trendall, A. F., J. R. de Laeter, D. R. Nelson, and Y. J. Bhaskar Rao, Further zircon U-Pb age data for the Daginkatte formation, Dharwar Supergroup, Karnataka craton, *J. Geol. Soc. India*, *50*, 25–30, 1997.

van der Heyden, P., A middle Jurassic to Early Tertiary Andean-Sierran arc model for the Coast Belt of British Columbia, *Tectonics*, *11*, 82–97, 1992.

Vasudev, V. N., B. Chadwick, A. P. Nutman, and G. V. Hedge, Rapid development of the Late Archaean Hutti schist belt, Northern Karnataka: Implications of new field data and SHRIMP U-Pb zircon ages, *J. Geol. Soc. India*, *55*, 529–540, 2000.

Viswanatha, M. N., Geological map of parts of the Kolar Greenstone belt, Karnataka, scale 1:50,000, Geol. Surv. of India, Bangalore, 1978.

Viswanatha, M. N., and M. Ramakrishnan, Kolar belt, in *Early Precambrian Supracrustals of Southern Karnataka*, edited by J. Swami Nath and M. Ramakrishnan, *Mem. Geol. Surv. India*, *112*, 221–245, 1981.

Walker, R. J., S. B. Shirey, G. N. Hanson, V. Rajamani, and M. F. Horan, Re-Os, Rb-Sr and O isotope systematics of the Archean Kolar schist belt, South India, *Geochim. Cosmochim. Acta*, *53*, 3005–3013, 1990.

D. Chardon and P. Choukroune, Centre Européen de Recherche et d'Enseignement de Géosciences de l'Environnement (UMR CNRS 6635), Université Aix-Marseille 3, BP 80, 13545 Aix-en-Provence Cedex 4, France. (chardon@cerege.fr; pchoukr@cerege.fr)

C. M. Fanning, Research School of Earth Sciences, Australian National University, Canberra ACT 0200, Australia. (mark.fanning@anu.edu.au)

M. Jayananda, Department of Geology, Bangalore University, Bangalore 560 056, India. (mjayananda@rediffmail.com)

J.-J. Peucat, Géosciences-Rennes (UMR CNRS 6118), Université Rennes 1, Campus de Beaulieu, 35042 Rennes Cedex, France. (Jean-Jacques.Peucat@univ-rennes1.fr)